UNIVERSITY OF GAZİANTEP
GRADUATE SCHOOL OF
NATURAL & APPLIED SCIENCES

FRICTION STIR WELDING OF DISSIMILAR ALUMINUM ALLOYS 2024 -T3 TO 6061-T6

M. Sc. THESIS
IN
MECHANICAL ENGINEERING

BY
NAZAR MUDHER ABDULWADOOD

JUNE 2013

Friction Stir Welding of Dissimilar Aluminum Alloys 2024-T3 To 6061-T6

M.Sc. Thesis
In
Mechanical Engineering
University of Gaziantep

Supervisor

Prof. Dr. Nihat YILDIRIM

By
Nazar Mudher ABDULWADOOD
June 2013

© 2013 [Nazar Mudher ABDULWADOOD]

T.C.
UNIVERSITY OF GAZİANTEP
GRADUATE SCHOOL OF
NATURAL & APPLIED SCIENCES
MECHANICAL ENGINEERING DEPARTMENT

Name of the thesis : Friction stir welding of dissimilar aluminum alloys 2024-T3 to 6061-T6

Name of the student : Nazar Mudher ABDULWADOOD

Exam date : 25.06.2013

Approval of the Graduate School of Natural and Applied Sciences

Assoc. Prof. Dr. Metin BEDIR
Director

I certify that this thesis satisfies all the requirements as a thesis for the degree of Master of Science.

Prof. Dr. Sait SÖYLEMEZ
Head of Department

This is to certify that we have read this thesis and that in our opinion it is fully adequate, in scope and quality, as a thesis for the degree of Master of Science.

Prof. Dr. Nihat YILDIRIM
Supervisor

Examining Committee Members	Signature
Prof. Dr. Ömer EYERCİOĞLU	
Assoc. Prof. Dr. Metin BEDIR	
Prof. Dr. Nihat YILDIRIM	
Assoc. Prof. Dr. Oguzhan YILMAZ	
Assist. Prof. Dr. Abdullah AKPOLAT	

I hereby declare that all information in this document has been obtained and presented in accordance with academic rules and ethical conduct. I also declare that, as required by these rules and conduct, I have fully cited and referenced all material and results that are not original to this work.

Nazar Mudher ABDULWADOOD

ABSTRACT

Friction stir welding of dissimilar aluminum alloys 2024-T3 to 6061-T6

Abdulwadood, Nazar Mudher

M.Sc. in Mechanical Engineering

Supervisor: Prof. Dr. Nihat Yildirim

June 2013, 82 pages

The importance of aluminum alloys 2024-T3 and 6061-T6 in the aerospace industrial applications push to use a new technology of joining process. The use of fusion welding process for these alloys with the temper conditions (T3 , T6) are not preferred because of the heat generated from the thermal cycle of the welding. Therefore, solid state nature of friction stir welding (FSW) will be very preferable for joining these dissimilar alloys. In the present study, an evaluation for the effect of process parameters on the microstructure and mechanical properties for dissimilar aluminum alloys 2024-T3 to 6061-T6 joint produced by FSW. The experimental work was carried out in the laboratory of mechanical engineering at Gaziantep University and in BCS Metal Company. In this study, FSW joints of good quality have been successfully fabricated from plates with 3mm thickness, using locally made friction stir tool. Four different rotational speed (600, 800, 1000 and 1200 rpm) and three different tool travel speeds (25, 75, and 100mm/min) were used. Experimental results showed that FSW results in fine and equiaxed grain structure at the nugget zone. Better tensile properties were obtained at rotation speed of 1000rpm and traverse speed of 50mm/min. Joint ductility was comparable to that of the base alloys. Tensile failure is found to occur at locations of lower hardness across the welded joints.

Keywords: Friction stir welding, dissimilar welding, aluminum alloy, mechanical properties, microstructure.

ÖZ

2024-T3 to 6061-T6 farklı aluminyum alaşımlarının sürtünme karıştırma kaynağı ile kaynaklanması

Abdulwadood, Nazar Mudher

Yüksek Lisans Tezi, Makina Mühendisliği

Tez Yöneticisi: Prof. Dr. Nihat Yildirim

Haziran 2013, 82 sayfa

2024-T3 ve 6061-T6 gibi farklı aluminyum alaşımlarının uzay ve havacılık alanlarındaki kullanımının yaygınlaşması kaynak işlemleri için yeni teknolojilerin kullanımını gerektirmektedir. Ergitme kaynak metodlarının, T3 ve T6 temperleme durumları ile birlikte kullanımı önerilmemektedir, çünkü kaynak esnasında oluşan ısı kaynağın ısıl işlem özelliğini etkilemektedir. Bundan dolayı bu alaşımların birleştirilmesinde, katı hal kaynak yöntemlerinden biri olan sürtünme karıştırma kaynağının (friction stir welding -FSW) kullanılması tercih edilmektedir. Bu çalışma kapsamında dönme hızı (deur) ve ilerleme hızının, sürtünme karıştırma kaynağı ile kaynaklanmış farklı iki malzeme olan 2024-T3 ve 6061-T6 aluminyum alaşımları için mikroyapı ve mekanik özellikleri üzerindeki etkilerini inceledik. Deneysel çalışmalar Gaziantep Üniversitesi, Makina Mühendisliği Bölümü Laboratuarında ve BCS Metal Sanayi Şirketi'nde gerçekleştirilmiştir. Bu çalışmada, 3 mm kalınlıktaki iki farklı malzeme (2024-T3 ve 6061-T6 aluminyum alaşımları), local olarak qeliştirile sürtünme karıştırma takımı kullanılarak yüksek kalitede başarılı bir şekilde kaynaklanmıştır. Dört farklı dönme hızı (600, 800, 1000 ve 1200 devir/dakika) ve üç farklı takım ilerleme hızında (25,75 ve 100 mm/dakika) çalışılmıştır. Deneysel sonuçlar göstermiştirki, sürtünme karıştırma kaynağı kaynak dolgu bölgesinde saf ve eş eksenli tane yapısı oluşturmuştur. En makul çekme özellikleri 1000 devir/dakika dönme hızı ve 50 mm/dakika ilerleme hızında elde edilmiştir. Kaynak sünekliliği malzemelerin kendi sünekliliği ile kıyaslanmış ve çekme hatasının kaynaklı kısım boyunca, sertlik değerinin minimum olduğu yerde meydana geldiği görülmüştür.

Anahtar Kelimeler: Sürtünme karıştırma kaynağı, farklı aluminyum alaşımlarının kaynakla birleştirilmesi, farklı birleşme yerlerinin mekanik özellikleri, mikroyapı

Dedication

I dedicated this work to my beloved Dad, Mother, Sister and my Wife, with my greatest appreciation for their endless love, support and encouragement .

ACKNOWLEDGEMENTS

First praise is to **ALLAH**, the Almighty, on whom ultimately we depend for sustenance and guidance. My sincere appreciation goes to my supervisor Prof. Dr. **Nihat YILDIRIM**, whose guidance, careful reading and creative comments was valuable. His timely and efficient contribution helped me shape this into its final form and I express my sincerest appreciation for his assistance in any way that I may have asked.

A special thank to University of Gaziantep for the real support and laboratory facilities. Also I want to thank **BCS Metal Company** (engineers and operators) for their assist to achieve this work. Also a special thank for Prof. Dr. Adnan Nama in Technical College Baghdad for the assistant and advising. Special thank to Research Asst. **Burak ŞAHIN**. And those who were directly or indirectly involved in the process of producing this research report, for their generous assistance, and to all my friends, for their support and giving me a suitable environment to study.

I would like to express my deep appreciation to my **father** and my **family**, to whom I dedicate my work. I am thankful for their love, which helped me in the successful completion of my study.

TABLE OF CONTENT

CONTENT ..... Page

ABSTRACT v

ÖZ vi

ACKNOWLEDGEMENTS viii

TABLE OF CONTENT ix

LIST OF FIGURE xiii

LIST OF TABLE XV

LIST OF SYMBOLS xvi

CHAPTER 1: INTRODUCTION 1

1.1 General 1

1.2 Principal of Friction Stir Welding 2

1.3 Friction Stir Welding Parameters 4

1.4 Objective of Study 6

1.5 Layout of thesis 6

CHAPTER 2: LITERATURE REVIEW 7

2.1 Introduction 7

2.2 Aluminum and its alloys 7

2.3 Friction Stir Welding of the 2024 Al alloys 9

2.3.1 The effect of FSW parameters on microstructure and mechanical properties of 2024 Al alloys 10

2.3.2 The effect of temper condition on the quality of friction stir weldments 12

2.3.3 Dissimilar welding of aluminum alloy 2024 13

2.4 Friction Stir Welding of the 6061 series Al alloys 14

2.4.1 The effect of FSW parameters on microstructure and mechanical properties of 6061 series Al alloys 15

2.4.2 The effect of temper condition on the quality of friction stir weldment 18

2.4.3 Dissimilar welding of aluminum alloy 6061 19

2.5 FSW of Dissimilar Al alloys of 2024 and 6061 23

CHAPTER 3: EXPERIMENTAL WORK 26

3.1 Introduction 26

3.2 Material used 26

3.3 Friction Stir Welding Tool 28

3.4 Friction Stir Welding operation 29

3.5 X-Ray radiographic test 33

3.6 Tensile Test 33

3.7 Bending Test 35

3.8 Microhardness Testing 37

3.9 microstructural evaluation of the weld area 38

CHAPTER 4: RESULTS AND DESCUSSION 41

4.1 Introduction 41

4.2 Effect of tilt angle on the joints fabricated by friction stir welding 41

4.3 Effect of rotational and travel speeds on the appearance of the weld 42

4.4 Radiography inspection.....43

4.5 The effect of process parameters on tensile properties 46

4.6 The effect of process parameters on bending properties.....56

4.7 Effect of welding conditions on microhardness profile of the weld area 59

4.8 Effect of welding conditions on microstructural features of the weld area 64

CHAPTER 5: CONCLUSIONS 72

5.1 Conclusion 72

5.2 Recommendation for future study.....74

REFERENCES.....75

APPENDIX A: The certificate of chemical composition 75

APPENDIX B: Radiographic test report 75

LIST OF FIGURES

Figure 1.1 Principle of friction stir welding.....3

Figure 1.2 A schematic that depicts the metal flow during FSW 3

Figure 2.1 Classification and application of aluminum alloys 9

Figure 2.2 Weldability of various aluminum alloys 10

Figure 2.3 Photograph of the tensile fractured.....20

Figure 2.4 Hardness profile of the cross-section area 22

Figure 2.5 Representative 2024 Al:6061 Al FSW microstructure Weld cross-section showing large tunnel and unwelded plate at weld bottom 24

Figure 3.1 (a) FSW tool used in the current study 28

Figure 3.1 (b) Schematic of FSW tool used in the current study.....29

Figure 3.2 The milling machine utilized for friction stir welding trials.....29

Figure 3.3 The digital scale used for rotating the head of the milling machine.....30

Figure 3.4 A close-up view of friction stir butt welding.....31

Figure 3.5 Shape and size of the square butt joints used in the current work.....32

Figure 3.6 Tinus Olsen universal tensile testing machine.....34

Figure 3.7 Tension test specimen geometry. Dimensions are in millimeters 35

Figure 3.8 Schematic of bending test specimen according to ASTM.....36

Figure 3.9 Bending device 36

Figure 3.9 (a) Zwick/Roell microhardness digital tester.....37

Figure 3.9 (b) Clause up view for the holding stage and indenter 38

Figure 3.10 The specimen of microstructure testing.....39

Figure 3.11 Optical microscope equipped with an eyepiece digital camera.....40

Figure 4.1 The appearance of the welds using 0˚ tilt angle 42

Figure 4.2 Appearance of the weld using cylindrical pin and variable rotation speed of:(a) 600rpm. (b) 800rpm. (c) 1000rpm. (d) 1200rpm at V of 50mm/min.....43

Figure 4.3 Appearance of the weld using cylindrical pin and variable welding speed of:(e) 25mm/min. (f) 75mm/min. (g) 100mm/min at ω of 1000rpm 44

Figure 4.4 X-ray radiographic test for the specimen 1,2,3,4.....45

Figure 4.5 X-ray radiographic test for the specimen 5,6,7,8.....46

Figure 4.6 (a) Stress-strain curve of base metal AA2024-T3 47

Figure 4.6 (b) Stress-strain curve of base metal AA6061-T6 48

Figure 4.6 (c) Stress-strain curve for the case of AA2024-T3 on advancing side using rotation speed of 600 rpm 49

Figure 4.7 Fracture locations for the case of (2024 alloy on advanced side) at the rotational speed of (a) 600rpm, (b) 800rpm, (c) 1000rpm and (d) 1200rpm with a constant traverse speed of 50mm/min.....50

Figure 4.8 Stress –strain curves for the case of AA 6061-T6 on advanced side using rotation speed 1000 rpm.....53

Figure 4.9 Fracture location for the case of (6061 alloy on advanced side) at the rotational speed of (e) 600rpm, (f) 800rpm, (g) 1000rpm and (h) 1200rpm with a constant traverse speed of 50mm/min.....54

Figure 4.10 Stress –strain curves for the case of AA 6061-T6 on advanced side and travel speed 75 mm/min.....55

Figure 4.11 fracture location for the case of (variable traverse speed of (i) 25mm/min, (j) 75mm/min and (k) 100 mm/min at a constant rotation speed of 1000 rpm 55

Figure 4.12 Face and root bending specimens 59

Figure 4.13 (a) bending specimens for the case of 2024-T3 on advancing side 59

Figure 4.13 (b) bending specimens for the case of 6061-T6 on advancing side.....60

Figure 4.13 (c) bending specimens for the case of using variable travel speeds 60

Figure 4.14 Vickers hardness profile across the weld centerline of friction stir welded Al alloy for different tool rotation and constant travel speeds of 50 mm/min 62

Figure 4.15 Vickers hardness profile across the weld centerline of friction stir welded Al alloy for different travel speeds and constant rotation speed of 1000 rpm 63

Figure 4.16 macrographic of FSW of the dissimilar joint showing microstructural zones.....66

Figure 4.17 Optical micrographs on a transverse section through a friction stir welded dissimilar alloys 2024-T3 and 6061-T6 at rotational speed of (a) 600 rpm, (b) 800 rpm , (c) 1000 rpm & (d) 1200 rpm at a constant traverse speed of 50 mm/min 68

Figure 4.18 Optical micrographs on a transverse section through a friction stir welded dissimilar alloys 2024-T3 and 6061-T6 at traverse speed of (e) 25 rpm, (f) 75 rpm & (g) 100 rpm at a constant rotational speed of 1000 rpm 69

Figure 4.19 microstructure comparisons of 2024-T3 and 6061-T6 (a) cross- sectional view of the weld, (b) base plate grain structure of 2024-T3, (c) grain structure of the nugget zone & (d) base plate grain structure of 6061-T6.....69

LIST OF TABLES

Table 1.1 Different friction stir welding tools designed at TWI ……..... 5

Table 2.1 Some physical properties of aluminum ……. 8

Table 2.2 Process parameters of the work …….. 15

Table 2.3 Welding parameters and designations of FSW AL6061-T651 …….. 16

Table 2.4 Tensile properties of FSW AL 6061-T651 joints ……..... 17

Table 2.5 Mechanical properties and fracture locations of the welded joints in transverse direction to the weld center line …… 19

Table 3.1 Chemical composition of the base metals(element concentration %) 27

Table 3.2 Mechanical properties of the base metals ……. 27

Table 3.3 Friction stir welding process parameters used to fabricate the joints … 33

Table 3.4 Second process parameters used to fabricate the joints…… 33

Table 4.1 Tensile test results of base metal ……..... 47

Table 4.2 Tensile test results of the weldments (2024 at advanced side) …… 48

Table 4.3 Tensile test results of the weldments (6061 at advanced side)…… 51

Table 4.4 Tensile test results of the weldments (variable traverse speed)……. 54

Table 4.5 (a) Microhardness distribution results using variable rotational speeds …… 64

Table 4.5 (b) Microhardness distribution results using variable traverse speeds 65

LIST OF SYMBOLS

FSW	Friction Stir welding
TWI	The Weld Institute
AA	Aluminum Association
NASA	National aeronautics and Space Administration
2xxx	Aluminum-Copper alloy series
6xxx	Aluminum-Zinc Mg-Si series
NZ	Nugget Zone
TMAZ	Thermo-Mechanically Affected Zone
HAZ	Heat Affected Zone
BM	Base Metal
HSS	High Speed Steel
H13	Hot worked tool steel
T3	Solution heat treatment, cold Worked, and naturally ageing
T6	Solution heat treatment, and artificial ageing
ASTM	American Society for Testing and Materials
AS	Advancing side of the weld
RS	Retreating side of the weld
PCBN	Polycrystalline Cubic Boron Nitride

AMCs	Aluminum Matrix Composite
AISI	American Institute for Steel and Iron
UTS	Ultimate tensile strength (Mpa)
σ_y	Yield strength (Mpa)
PC	Personal Computer
USP	Universal Serial Bus
CW	Clock wise direction
V	Tool Travel Speed (mm/min)
ω	Tool Rotation Speed (rpm)
θ	Tilt angle (degree)

CHAPTER 1

INTRODUCTION

1.1 General

Friction stir welding (FSW) is a solid-state joining process that has been invented at The Weld Institute (TWI, United Kingdom), and patent in 1991 by Wayne Thomas under research funded by in part by the National Aeronautics and Space Administration (NASA) (Wayne Thomas, 2011) . It is an adaptation of the friction welding process. FSW is a continuous process that involves plunging a specially shaped rotating tool between the butting faces of the joint. The relative motion between the tool and the workpies generates frictional heat that creates a plasticized region around the immersed portion of the tool. The shoulder prevents the expelled of metal from the weld region. The tool is moved relatively along the joint line, pushing the plasticized material to coalesce behind the tool to form a solid–phase joint (Akinlabi, Esther Titilayo, 2010) .Since its invention, the process has received world-wide attention, specialized companies from Europe, Japan and USA are using the technology in production (C. J. Dawes, 1999). It can be used also for welding aluminum alloys of different alloy groups or yet dissimilar materials, metal matrix composites and plastics.

Other materials such as magnesium, copper, zinc, titanium and even steel can be welded with this process. The process provides better properties than the conventional arc welding processes, at most for aluminum alloys. Difficulties related to sensitivity to solidification cracking, gas porosity caused by the

hydrogen absorbed during welding and thermal distortion, very common in fusion welding processes, do not happen in this process. Also the process provide relatively good strength and ductility along with minimization of residual stress and distortion, no consumables required, no fumes or the spatter which mean safety improvements, can operate in all positions (horizontal, vertical, etc), easily automated on simple milling machines (J. Norberto Pires, 2006). The ever growing list of FSW users includes Boeing, Airbus, Eclipse, NASA, US Navy, Mitsubishi, Kawasaki (Calvin Blignault). FSW technique can be applied effectively to a variety of joints configurations like butt joints, lab joints, T butt joints and even fillet joints (C. J. Dawes, 1999).

1.2 Principal of Friction Stir Welding

The principal of friction stir welding is illustrated in figure 1.1. This process consist of plunging a tool rotating at a constant speed into the joint line between two butted pieces of plate, until the tool shoulder comes into contact with the working surface, the tool is moved at a constant traverse speed along the line of joint, the tool have a profiled probe or pin and shoulder (Gene Mathers, 2002). The probe length being slightly less than the depth of the weld required. The purpose of the tool is heating the joint portion of the plates and moving the material. The heat causes to softening the material and the relative motion of rotation and transverse leads to drag the material from the front portion of the pin to the rear of it which is resulting to produced the joint (R.S. Mishra, 2005).

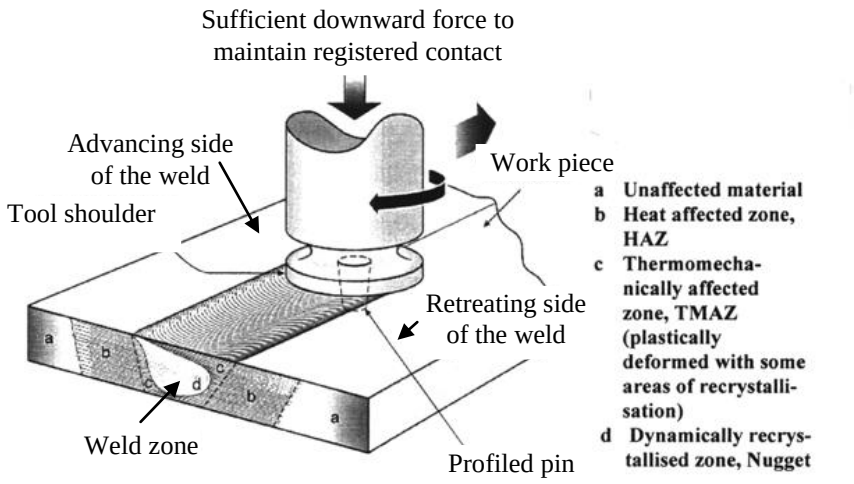

Figure 1.1 Principle of friction stir welding (L. Boehm, 2004)

The metal in the working zones is forced both upwards into the zone of the shoulder and downwards into the zone of extrusion as shown schematically in figure 1.2. In the extrusion zone, the metal flows around the pin from the front to the rear. Adjacent to the extrusion zone is the forging zone where metal lying ahead to the rotating and translating tool is forced into the cavity left behind the forward moving pin. The advancing side (AS) is the side where the direction of the tool rotation and traverse direction are the same and the side where the velocity vectors are opposite is referred as retreating side (K.Kumar, Satish V. Kailas, 2007).

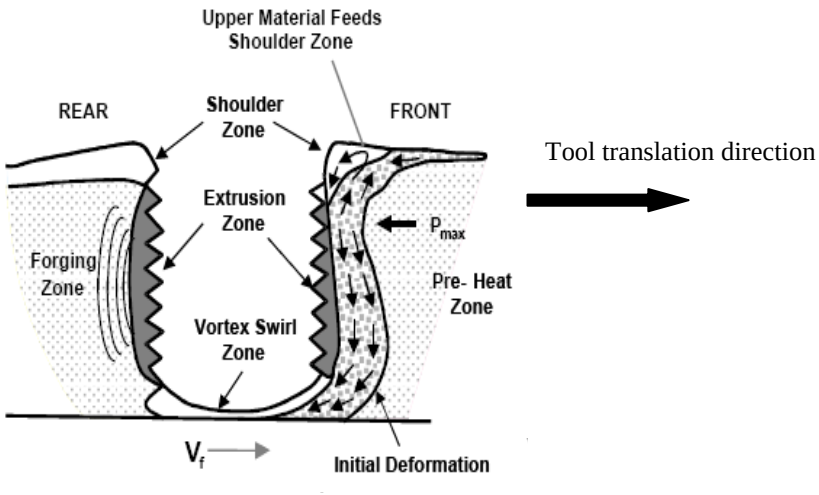

Figure 1.2 A schematic that depicts the metal flow during FSW (Brad Richards).

1.3 Friction Stir Welding Parameters

In order to provide high quality welds, some parameters should be controlled for a successful outcome. Rotational and travel speeds, tool design and joint configuration have an important effect on the material flow and the temperature distribution. (Akinlabi, Esther Titilayo, 2010). FSW tool design, which includes material selection and geometry, is one of the most important factors that influence the quality of the weld and the maximum possible welding speed. Tool materials, affect friction coefficients and heat generation, while, Tool configuration influences joint size and profile (Terry Khaled, 2005). Selecting the correct tool material requires the knowledge of material characteristics that are important for each friction stir application. Polycrystalline cubic boron nitride (PCBN) and W based alloys are commonly used tool materials for FSW of harder alloys, Materials such as aluminum or magnesium alloys and aluminum matrix composites (AMCs) are commonly welded using steel tools (R.Rai, 2011). Hot-worked tool steel, such as AISI H13 has proven acceptable for welding a wide range of materials (Akinlabi, Esther Titilayo, 2010). Friction stir welding is carried out around 70-90% of the material melting point so it is important that the material grade of the welding tool must be such that its strength, hot hardness and toughness can be maintained at temperatures as high as it can ensure workpiece softening during welding process otherwise the tool can wear or twist and break. Threaded pins were found to assist in ensuring that the plastically deformed workpiece material is fully delivered around the pin. Threaded and fluted pins and frustum pins with flats were also found to enable higher speeds, more thorough mixing and better quality welds (Terry Khaled, 2005) **.** Several tools designed at TWI are shown in table1-1 (Akinlabi, Esther Titilayo, 2010).

Table 1.1. Different friction stir welding tools designed at TWI.

Tool	Cylindrical	Whorl™	MX triflute™	Flared triflute™	A-skew™	Re-stir™
Schematics						
Tool pin shape	Cylindrical with threads	Tapered with threads	Threaded, tapered with three flutes	Tri-flute with flute ends flared out	Inclined cylindrical with threads	Tapered with threads
Ratio of pin volume to cylindrical pin volume	1	0.4	0.3	0.3	1	0.4
Swept volume to pin volume ratio	1.1	1.8	2.6	2.6	Depends on pin angle	1.8
Rotary reversal	No	No	No	No	No	Yes
Application	Butt welding: fails in lap welding	Butt welding with lower welding torque	Butt welding with further lower welding torque	Lap welding with lower thinning of upper plate	Lap welding with lower thinning of upper plate	When minimum asymmetry in weld property is desired

There are different shoulder profiles designed in TWI for different applications, the underneath view of the shoulder have a flat or grooved (spiral or scrolls) or concave shape which considered as the mostly preferred (R.S. mishra, 2005). In FSW, two welding parameters are very important: tool rotational speed (rpm) in clockwise or counterclockwise direction and tool traverse speed (mm/min). The rotation speed influence the heat generated in the weld area. On the other hand, tool travel speed influences the heat input per unit weld length, and the amount of specific heat input decreases with increasing travel speed. Improper combination of tool rotation and travel speeds can be detrimental to the weld region and can lead to the formation of several kinds of defects. Insufficient welding temperature due to low tool rotation speed or high tool traverse speed, for example, means that the weld material is unable to accommodate the extensive deformation during welding. This may result in long, tunnel like defects running along the weld which may be surface or subsurface. Another welding parameters have more significant effect are the tool tilt angel (θ), it causes the rear of the tool shoulder to be plunged more into the surface of the plates than the front edge, thus allowing gradual increase of the contact pressure on the top

surface of the plates behind the tool pin. This pressure leads to forging the material at the rear of the tool resulting in better weld quality when compared with situations where zero tilt angle (P. Kah, 2009).

1.4 Objective of study

The objective of this study is to evaluate the effect of friction stir welding parameters including rotation speed, traverse speed, tilt angle and the location of the alloys on the microstructure and mechanical properties of the specific dissimilar aluminum alloys 2024-T3 and 6061-T6 using variable range of rotational and traverse speeds.

1.5 Layout of Thesis

The contents of each chapter can be explained as follows:

Chapter 1 Introduction: Introducing a brief history of friction stir welding as well as explaining the principal objectives and layout of the thesis.

Chapter 2 Literature Review: This chapter covered previous work that deals with, friction stir welding of aluminum alloys 2024 and 6061 in general, dissimilar welding of these alloys in particular, process parameter effecting the quality of weld .

Chapter 3 Experimental Work and Methodology: This chapter gives a description of the experimental apparatus, models and procedures.

Chapter 4 Results and Discussion: This chapter gives results and discussions, analysis of the data obtain from experiments with some comparisons with the other studies.

Chapter 5 Conclusion: the principal conclusions drawn from the results of the study and recommendation for future studies are present in this chapter.

CHAPTER 2

LITERATURE REVIEW

2.1 Introduction

Many researchers have focused on FSW of the aluminum alloys 2xxx and 6xxx series in general and aluminum alloys 2024 and 6061 in particular, dissimilar welding of these alloys with the other aluminum alloys and materials are studied also. Most of these studies investigated the effect of the process variables on the quality of the weld. These studies are presented in the following paragraphs.

2.2 Aluminum and its alloys

The existence of aluminum (Al) was postulated by Sir Humphrey Davy in the first decade of the nineteenth century and the metal was isolated in 1827 by Friedrich Wöhler. Aluminum is a relatively soft, durable, lightweight and ductile. It has an appearance ranging from silvery to dull gray. It is nonmagnetic. The yield strength of pure aluminum is 711 MPa, while aluminum alloys have yield strengths ranging from 200 to 600 MPa.

Table 2.1 shows some physical properties of aluminum. The method of extraction was invented simultaneously by Paul Heroult in France and Charles M. Hall in the USA and this basic process is still in use today. The resulting pure metal is relatively weak and as such is rarely used, particularly in constructional applications.

Table 2.1 some physical properties of aluminum

Properties	
Crystal structure	FCC
Density	2.70 $g \cdot cm^{-3}$
Melting point	660.32 °C
Thermal conductivity	237 $W \cdot m^{-1} \cdot K^{-1}$
Young's modules	70 GPa

To improve the mechanical strength, the pure aluminum is generally alloyed with metals such as copper, manganese, magnesium, silicon and zinc as it is shown in the figure 2.1. The importance of aluminum based on characteristics such as low density, good corrosion resistance, reasonably good strength and ductility, ease of fabrication, modern metallurgical control of structure and properties, and favorable economy, lead to consider it as a tonnage metal, second only to steel as a major factor in the metal industry

Aluminum and its alloys are available in a variety of cast and wrought forms and conditions of heat treatment. The common wrought forms are forgings, solid, hollow and tube extrusions, sheets, plates, strips, foils and wires, whereas castings are available in sand, pressure and gravity die cast forms.

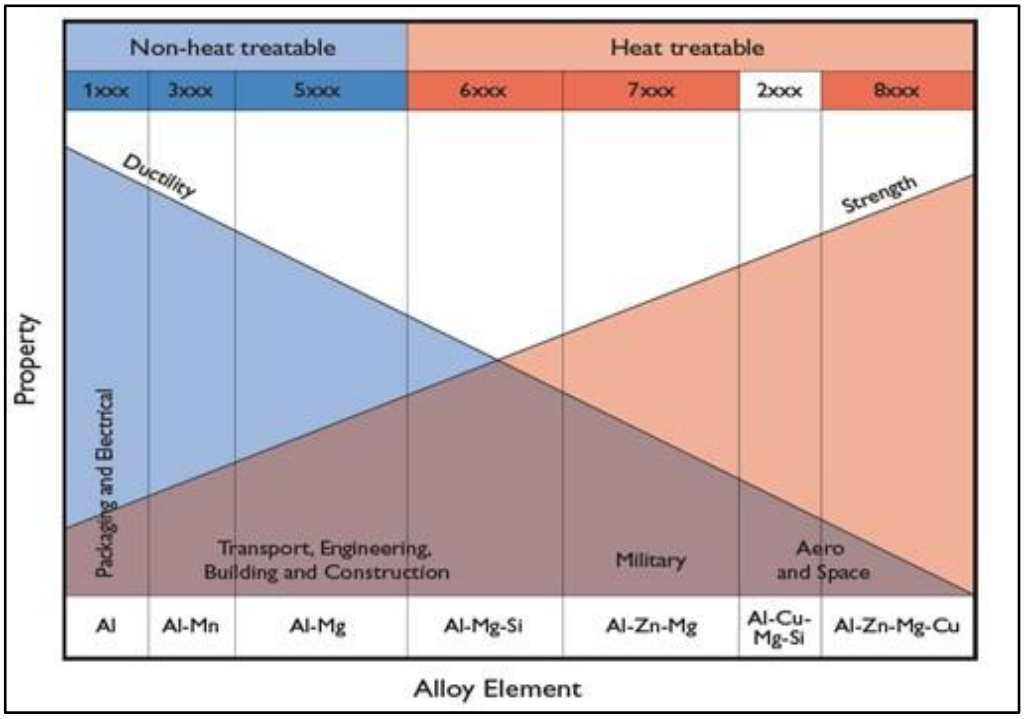

Figure 2.1 Classification and application of aluminum alloys (Thomas, W.M 1991)

2.3 Friction Stir welding of the 2024 aluminum alloys

For the applications requiring very high strength plus high fracture toughness, the aluminum alloy (2024) is the suitable one of the Al (2xxx) series which used specially for the aerospace and aircraft structures. The use of conventional fusion welding for the 2024 aluminum alloy is very difficult and do not provide high strength bond , for this reason Sustained research efforts during the last three decades have led to the invention of friction stir welding process as an applicable solid state joining technique, Figure 2.2 show the verity of aluminum alloys and their weldabilitys**.**

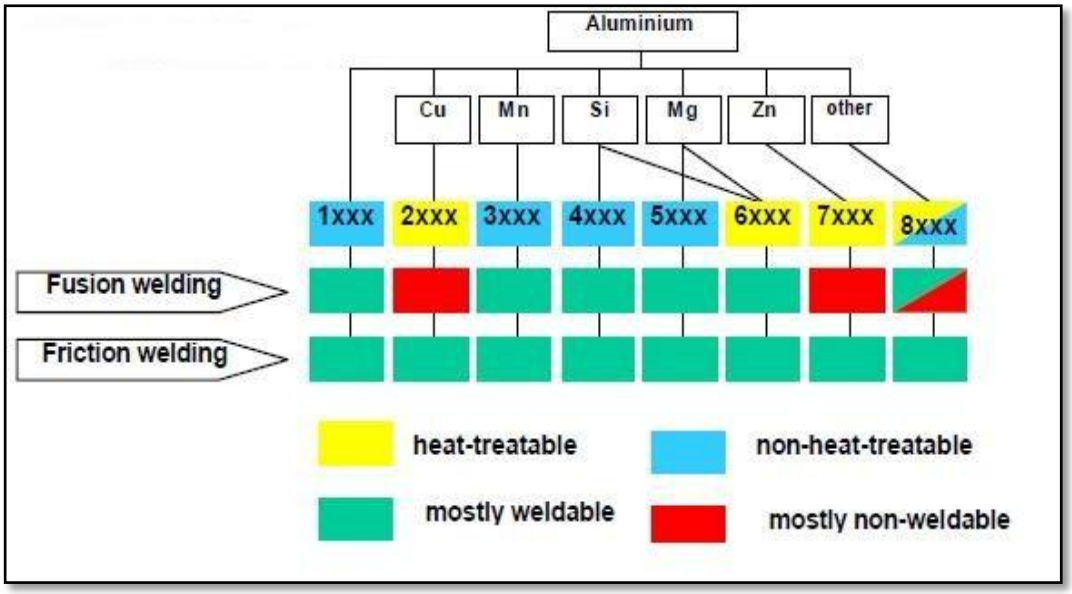

Figure 2.2 weldability of various aluminum alloys (Thomas, W.M 1991)

2.3.1 The effect of FSW process parameters on microstructure and mechanical properties of 2024 Al alloys

In order to satisfy a high quality weld many process parameters such as tool design, rotational speed, travel speed, tool tilt angle and material condition should be controlled. Many studies have focused on FSW process parameters and its effect on the mechanical properties of the 2024 aluminum alloy. These studies will be presented in the following paragraphs.

Nakata et al (2000) reported that excessively high tool rotational speed during friction stir welding of 4mm thick 2024-T6 alloy, leads to surface tearing and inner defects that has been attributed to grain boundary liquation due to melting of the comparatively low melting eutectic constituents. Nakata and his co-workers observed that post weld artificial ageing decreased the tensile strength of the alloy 2024-T6. Joint efficiency of about 80% to that of the parent metal in terms of tensile strength has been reported. They proposed an optimum revolutionary pitch between 0.2 and 0.3mm/rev.

Bahemmat et al (2008) studied the effect of rotational speed and tool pin profile on the mechanical properties of butt joints of 2024-T6 Al alloy. In this study, they used two pin profiles; one is threaded conical and the other is four-flute at different tool rotational speeds between 300 and 1000rpm.Their results showed that joints fabricated using the four-flute pin profile exhibited superior tensile properties compared to the threaded conical pin profile, irrespective of tool rotational speed.

Sutton M. A. et al. **(**2001**)** studied the microstructural changes of friction stir welds in 2024-T351 aluminum alloy. The measured process parameters were a rotational speed of 360 rpm and a travel speed of 198 mm/min. The nugget, has a refined microstructure. At the edge of the welding tool's pin, an abrupt transition occurs from the highly refined, equiaxed, grains comprising the nugget to deformed base metal grains. At a location corresponding to approximately the tool shoulder radius on the advancing side, a relatively coarse, recrystallized grain structure was observed. At 4.5 mm from the edge of the shoulder, the microstructure appears to b e similar to the original, elongated grain structure present in the rolled, 2024-T351 base material. As one travels from the crown to the root of the FSW, the grain size decreases, most likely due to the higher heat input near the crown that causes additional grain growth in this region.

2.3.2 The effect of base metal temper condition on the quality of friction stir weldments

Many of the previous studies has focused on the effect of the process parameters on the welding properties , the following studies presenting the effect of base metal temper condition on the FSW behavior of the 2024 series Al-alloys.

V. Dixit (2006) studied the effect of initial temper on the mechanical properties of friction stir welded Al-2024 alloy, Al-2024 alloy under two different initial tempers, T3 and T8, was used in this study. The results show the effect of initial temper appeared to exist mainly in the HAZ of the friction stirred specimens. In the processed T3 material, extremely fine S phase precipitates were observed, similar to those originally present in parent T8 material, in the HAZ region, tensile strength increased at higher heat index values for friction stirred T3 material, It was also noted that properties in the HAZ region of the processed T3 material were significantly higher than corresponding tensile properties at nugget and unprocessed regions for both initial tempers.

Hakan Aydin et. al. (2008) studied the effect of the base material temper condition of the alloy 2024 on the mechanical properties of the friction stir welded joints. They used four temper conditions for the alloy namely 2024-O, 2024-W, 2024-T4, and 2024-T6. They used a cylindrical tool with a conical threaded pin rotating at 2410rpm, traveling at 40mm/min and tilting angle 2-3°. In this investigation, they concluded that the mechanical properties of the friction welded joints affected by the temper condition of the base metal. They observed that the material in the O condition reach a strength higher than it for the other temper conditions.

2.3.3 Dissimilar welding of aluminum alloy 2024

The absence of dissimilar welding can be found widely in the new industrial application specially for the aluminum alloy, the difficulties of bonding dissimilar alloys to each other lead to use the qualified welding techniques, the following paragraphs focusing on the welding of AA 2024 to the other alloys .

P. Cavaliere (2008) analyzed the effect of process parameters on the mechanical and microstructural properties of dissimilar AA6082–AA2024 joints. The welding speed varying as 80 and 115 mm/min while the rotating speed was fixed at 1600 rpm . The position of the alloys was varying also on the advancing and the retreating side of the tool. The results showed that the highest values of microhardness are reached when the 2024 alloy is on the advancing side and the welding speed is 115 mm/min. The tensile strength increases by increasing the weld speed. The ductility is higher with increasing the weld speed in the case of AA6082 on the advancing side, while it decreases in the case of AA2024 on the advancing side. The best conditions of strength and ductility are reached in the joints welded with AA6082 on the advancing side and an advancing speed of 115 mm/min. the fatigue strength increases as the welding speed increases.

M. Vural (2007) studied the friction stir welding capability of aluminum alloys EN AW 2024-0 and EN AW 5754-H22. In this study they used a range of welding speed between 5-15 mm/min and a constant rotational speed of 2000 rpm. The results showed that these two aluminum alloys can be friction stir welded. The welding performance of EN AW 2024-0 is reached to 96.6 % and the hardness value in the weld area is increased about 10- 40 Hv. It is possible to perform dissimilar welding for the aluminum alloys EN AW 2024-0 and EN AW 5754-H22 and the weld performance is reached a value of 66.39%.

Saad and Toshiya (2007) Studied the Microstructure and Mechanical Properties of Friction Stir Welded Dissimilar Aluminum Joints of AA2024-T3 to AA7075-T6. The travel speed used is 100 mm/min and the rotation speeds between 400 and 2000 rpm. The effects of rotation speeds on the microstructures of the stir zone (SZ), hardness behavior, and tensile strength of the joints were evaluated. The results showed that

no mixing in the SZ at the lowest rotation speed of 400 rpm. The increasing in rotation speed more than 400 rpm lead to form a mixed structure likewise onion ring with a change of equiaxed grain size. The hardness increased in the zones of aluminum alloy 2024-T3. At 2000 rpm the hardness of SZ mainly depend on the material fixed at the advancing side. The minimum hardness was in the (HAZ) on the side of AA2024-T3 Al alloy. For the tensile test results, fractured located at the HAZ on 2024-T3 side and a maximum tensile strength of the joints was achieved at 1200 rpm when 2024-T3 Al alloy was located on the advancing side. On the other hand, the tensile properties of SZ showed higher values when 7075 Al alloy was located on the advancing side.

2.4 Friction stir welding of 6061 series Al alloys

Aluminum alloy 6061 plays major role in the aerospace industry in which magnesium and silicon are the principal alloying elements. It is widely used in the aerospace applications because it has good formability, weldability, corrosion resistance and good strength. When using the arc welding techniques, long butt or lap joints between AA 6061 and other aluminum alloys are difficult to make without distortion because of high thermal conductivity. The feasibility of joining aluminum alloy 6061 by (FSW) technique lead to use it as a new technology.

2.4.1 The effect of FSW process parameters on microstructure and mechanical behavior of 6061 Al-alloys

Many researchers tried to study the friction stir welding process and most of them focused on the geometrical and operational parameters, below are some of these studies for aluminum alloys 6061.

Won-Bae Lee (2004) investigated the microstructural change related with the mechanical properties of a friction stir welded aluminum alloy 6061-T6 under

various welding conditions. the tool rotation speed and welding speed were taken into account and changed from (1250 rpm) to (3600 rpm) and from 87mm/min to 267mm/min, respectively, the angle of the tool was 3°. They found that when the rotation speed was 1250 rpm at 267mm/min welding speed, some voids was exist in the weld zone, the grain size in the SZ increases with increasing rotation speed and decreasing welding speed. The grain size shows about 22 mm at the condition of 1250 rpm, 267mm/min, and 40 mm at the condition of 3600 rpm, 267mm/min. The UTS, YS and elongation for the condition of 3600 rpm of rotation speed (including large void in the SZ), of the joints are approximately 200 MPa, 80 MPa and 10% respectively.

M. A. Abdelrahman (2012) studied the effect of FSW tool geometry on AA6061-T6 weldments, they used several FSW tools (differ from each other in pin angle, shoulder diameter, and shoulder concavity) to fabricate a number of joints, the table 2.2 shows the process parameters relating to the tool geometry and the operational variables, It was found that the FSW tool with tapered cone pin, concave shoulder, and shoulder diameter equal to four times the welded plate thickness is suitable to produce a sound weld.

Table 2.2 Process parameters of the work (M. A. Abdelrahman, 2012)

	Joint 1	Joint 2	Joint 3	Joint 4	Joint 5
Plate thickness mm	11	11	11	11	5.3
FSW tool	Tool 1	Tool 1	Tool 2	Tool 3	Tool 4
Tool sink depth mm	0.1	0.1	0.1	0.1	0.1
Tilt angle	0°	0°	0°	2°	2°
Rotation rate rpm	1120	1120	1120	1120	1120
Traverse speed mm/min	22.4	90	22.4	22.4	22.4

F.C. LIU and Z.Y. MA (2008) studied the effect of tool geometry and Welding Parameters on Microstructure and Mechanical Properties of Friction-Stir-Welded 6061-T651 Aluminum Alloy, they used a tools with the shoulders of 16, 20, and 24 mm in diameter and the threaded conical pins of 8 and 6 mm in root diameter, rotation speed varying form 900, 1200 and 1400 rpm while the welding speed were 200, 400 and 600 mm/min as illustrated in table 2.3.

Table 2.3 welding parameters and designations of FSW AL6061-T651 (F.C. LIU and Z.Y. MA 2008)

Sample	Shoulder Diameter (mm)	Pin Diameter (mm)	Rotation Rate (ω), rpm	Welding Speed (v), mm/min	Designation
1	16	8	1400	400	16-8-1400-400
2	20	8	1400	400	20-8-1400-400
3	24	8	1400	400	24-8-1400-400
4	24	8	1400	600	24-8-1400-600
5	24	8	1400	200	24-8-1400-200
6	24	8	1200	200	24-8-1200-200
7	24	8	900	200	24-8-900-200
8	20	6	1400	400	20-6-1400-400

The results show that the shoulder diameter of 16 mm exhibited a rectangular SZ with an incomplete onion ring structure, With increasing the shoulder diameter, the SZ changed from rectangular to elliptical, increasing the welding speed from 400 to 600 mm/min, the center of the onion rings shifted from the middle of the SZ to the upper part, whereas decreasing the welding speed from 400 to 200 mm/min, the onion ring structure disappeared, When the pin diameter decreased from 8 to 6 mm, the size of the SZ decreased obviously, The tensile properties of the FSW 6061Al-T651 joints are shown in the Table 2.4 which is reveal four important findings. First, similar elongation for all the welds. Second, increasing the shoulder diameter or the pin diameter did not produce an effect on the tensile strength. Third, the tensile

strength increased with increasing the welding speed. Fourth, increasing the rotation rate did not change the strength of the welds.

Table 2.4 Tensile properties of FSW AL 6061-T651 joints (F.C. LIU and Z.Y. MA 2008)

Designation	UTS, MPa	El., Pct	UTS_{FSW}/UTS_{base}
16-8-1400-400	231	8.1	0.75
20-8-1400-400	229	8.4	0.74
24-8-1400-400	230	8.3	0.75
24-8-1400-600	243	8.6	0.79
24-8-1400-200	214	8.8	0.69
24-8-1200-200	211	8.6	0.69
24-8-900-200	214	8.4	0.69
20-6-1400-400	230	8.2	0.75

Huijie LIU. et. al. (2005) Examined the Friction Stir Weldabilities of the strain-hardened AA 1050-H24 and precipitate-hardened AA6061_T6 aluminum alloys. They used rotation speed of 100-1500 rpm and welding speed of 100-1000mm/min. Their observations also revealed the maximum tensile strength efficiency of the AA1050-H24 joints is similar to that of AA6061-T6 joints, the effective range of welding parameters for AA1050-H24 is limited, while for AA6061-T6 is wide, the AA1050-H24 have smooth surface ripples of the weld ,no elliptical nugget in the weld and no interface between the SZ and the thermomechanically affected zone, for the AA6061-T6 the weld surface slightly rougher, an elliptical nugget exist and there is an interfaces among the weld nugget and for the both of the alloys there was an internal defect looks like long crack located in the lower part of the weld .

2.4.2 The effect of base metal temper condition on the quality of friction stir weldments

Many of the studies and researches has focused on the effect of the base metal temper condition on the FSW behavior of aluminum-magnesium silicon alloy 6061.

N. T. Kumbhar and K. Bhanumurthy (2008) studied the Friction Stir Welding of Al 6061 Alloy. The tool rotation speeds used in this study were 710, 1120 and 1400 rpm and the traverse speeds are 63, 80 and 100 mm/min. The tool tilt angle 2°. The result show that Defect free joints could be obtained for lower rotation speed 700 rpm and with a high travel speed of 80 mm/ min. On the other hand it is essential to have a minimum of 1000 rpm for Al 6061-T651 condition to obtain similar welding speeds. The lower hardness (38 VHN) of the 0-condition alloy leads to the possibility to stir this alloy at lower rotation speeds and at higher welding speeds.

Indira Rani M (2011) Studied the optimization of FSW parameters in different conditions of base material and the microstructures of the as-welded condition are compared with the post weld heat treated microstructures welded in annealed and T6 condition of AA6061. They used different process parameters 800 rpm, 15 mm/min and 800rpm, 10 mm/min, The microstructure studies aimed at characterization of either the shape and dimensions of the grains across the joint for different kinds of conditions(annealed and T6) of Al alloy. They observed that for annealed condition the rotation speed 800 rpm and welding speed 10 mm/min and 15 mm/min are the optimal parameters, while for the ‘T6’ condition rotation speed of 1000 rpm and welding speed 10 mm/min are the optimal parameters.

2.4.3 Dissimilar welding of aluminum alloy 6061

Higher-strength aluminum-magnesium silicon alloy extrusions and plate welded with the other alloys in widely range, here are some of the studies published on this issue:

Muhamad Tehyo. Et. al. (2012) investigate the effect of welding parameters on the microstructure and mechanical properties of friction stir welded butt joints of dissimilar aluminum alloys between Semi-Solid Metal (SSM) 356-T6 and AA6061-T651, Aluminum alloy 6061-T651 were located on the retreating side and SSM356-T6 located on the advancing side. For this experiment, the rotation speeds are 1,750 and 2,000 rpm at a variable traverse speeds of (20, 50, 80, 120, 160, and 200 mm/min). The results of the investigation can be seen clearly in the table 2.5. Tensile elongation was generally greater at greater tool rotation speed. An averaged maximum tensile strength of 206.3 MPa was derived from a welded specimen produced at the tool rotation speed of 2,000 rpm associated with the welding speed of 80 mm/min.

Table 2.5 Mechanical properties and fracture locations of the welded joints in transverse direction to the weld center line (Muhamad Tehyo. Et. al. 2012)

Tool rotation speed (rpm)	Welding speed (mm/min)	Tensile properties at room temperature		
		Tensile strength (MPa)	Elongation (%)	Fracture location
1,750	20	193.5	5.071	TMAZ of SSM356-T6
	50	196.3	4.952	TMAZ of SSM356-T6
	80	192.8	5.289	TMAZ of SSM356-T6
	120	189.6	3.609	TMAZ of SSM356-T6
	160	181.1	2.389	TMAZ of AA6061-T651
	200	180.7	2.007	
2,000	20	202.1	4.006	SZ
	50	205.8	5.036	TMAZ of AA6061-T651
	80	206.3	5.519	TMAZ of SSM356-T6
	120	197.2	4.563	TMAZ of SSM356-T6
	160	198.7	4.748	SZ
	200	194.7	3.224	SZ

M. Ghosh. et. al. (2010) studied the Optimization of friction stir welding parameters for dissimilar aluminum alloys 6061-T6 and wrought A356 , they used rotational speed of 1000–1400 rpm and traversing speed of 80–240 mm/min, keeping other parameters same. It has been found, that interface microstructure within the weld nugget is dominated by retreating side alloy. Processing at low tool rotation and

traversing speed result in fine grain size of 6061 alloy near interface, reduce residual thermal stress, decrease extent of recovery– recrystallization. For the tensile properties of the joints the highest bond strength has been achieved for the 1000 rpm and 80 mm/min where it is close to the tensile strength of 6061 alloy, while the weakest joining was at 1400 rpm and 240 mm/min .

W H Jiang and R Kovacevic (2004) studied the feasibility study of friction stir welding of 6061-T6 aluminum alloy with AISI 1018 steel, they used tool with a shoulder and pin, 25mm and 5.5mm in diameter respectively, it was made of an H13 tool steel, The rotational speed of the tool was 914 r/min and its traverse speed was 140mm/min. the results show No cracks and porosity are visible, indicating a good quality. It can be seen that the hardness distribution is not uniform within the nugget. In some locations it is very high, even higher than that of the base steel, while in other locations it is lower, similar to that of the base Al alloy. The tensile test demonstrates that fracture occurred at the boundary between the nugget and the TMAZ in the base Al alloy rather than along the weld interface as shown in figure 2.3.

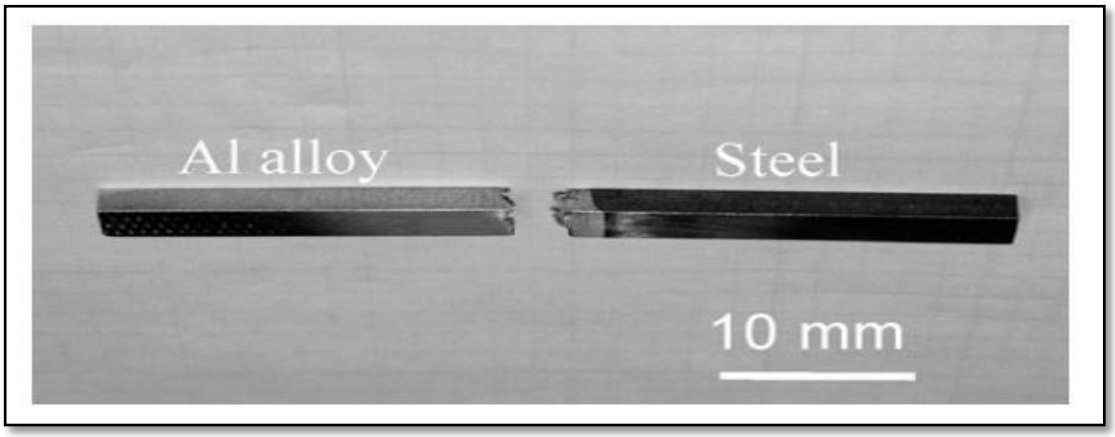

Figure 2.3 Photograph of the tensile fractured (W H Jiang and R Kovacevic. 2004)

Ki-Sang Bang. et. al (2011) . Studied the microstructure and mechanical properties of dissimilar 6061-T6 aluminum and Ti-6%Al-4%V joints fabricated by friction stir welding. The tool shape was circular cone of tapered pin from 6mm at the root area to 4mm at the tip of the probe with a screw. The shoulder diameter and probe length is 15mm and 4.5 mm, respectively. The tool was made of standard steel (SKD61). The travel speed used was 2.5 mm/s and the rotation speed was 1000 rpm, tilt angle was 3˚ and a plunge depth of 0.2mm.

Mechanical properties and microstructure were evaluated using tensile test, hardness test, optical microscopy, scanning electron microscope (SEM) and scanning transmission electron microscopy, respectively. Root portion of the stir zone (SZ) reveals a mixture of finely recrystallized grains of Al and Ti particles. The joint interface of tip area of probe was relatively flat. It is considered that the insufficient stirring due to inclined side of the probe was contributed to the decrease of weld strength.

Hardness profile for the welding cross-section evaluated by Vickers hardness tester and it is illustrated that the hardness level of Ti-6Al-4V alloy side was 350 HV. hard decrease of hardness level generated at the stir zone. Hardness level of SZ is slightly smaller than that of aluminum alloy base metal, except when the indenter hited tatinum particles. HAZ has a lowest hardness level. The ultimate tensile strength reached 134 Mpa representing 35% by that of aluminum alloy base metal. The all joints expressed lower strength and elongation than base metal. This is because probe tip area could not be affected by probe stirring action. The all joints are fractured in the weld region during transverse tensile test.

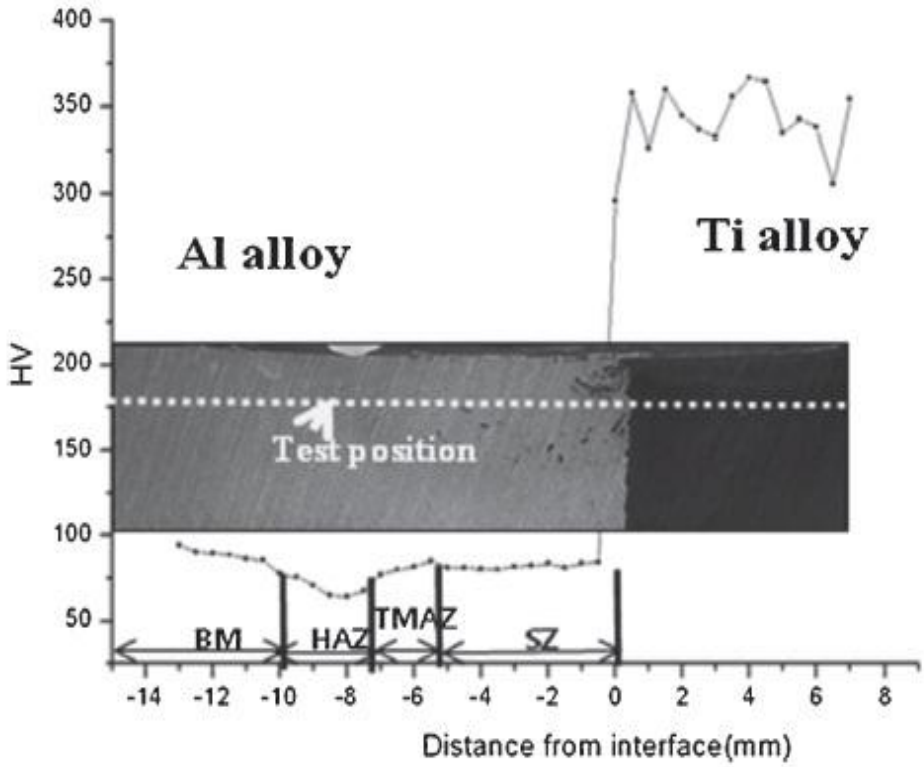

Figure 2.4 Hardness profile of the cross-section area (Ki-Sang Bang. et. al 2011)

P M G P Moreira. et. al. (2004) . Made an experimental characterization and computational modelling analysis of dissimilar FSW butt joints performed between aluminium alloys AA6061-T6 and AA6082-T6, The work included microstructure examination, microhardness, tensile and bending tests of all joints. The residual stresses generated during the FSW process were estimated. The used plate is 3mm thick, the travel speed was 224mm/min, tilt angle of 2.5º, rotating speed of 1120rpm. The tool geometry consists of threaded pin, smooth shoulder and concave at 7º with 17mm diameter. The results show that fracture occurred near the weld edge line, corresponding to the interface between the thermo-mechanically affected zone (TMAZ) and the heat affected zone (HAZ) and characterized by the lowest hardness. The dissimilar weld specimens presented an intermediate behavior although the smallest elongation value and the ultimate stress very close to the welded AA6082-

T6. The lower stress was observed at the nugget zone. A maximum residual stress value of 91,7MPa at the root surface of the tool shoulder, whereas in the same region but at the top surface of the weld bead the stress reaches 36,4MPa. The lower values occur at the aluminum alloy 6082-T6 side.

2.5 FSW of Dissimilar Al alloys of 2024 and 6061

Dissimilar welding of the materials being very important in the new industrial application .The friction stir welding of dissimilar materials is more complicated than similar materials due to difference in the physical, thermal, chemical and mechanical properties of base materials.

Ying Li. et.al. (1999) studied the flow visualization and residual microstructures associated with the FSW of 2024-T4 aluminum to 6061-T6 aluminum with 6.5mm thick, the tool rotation speed between 400 and 1200 rpm and the actual welding or traverse speed was constant at 60mm/min, tool tilt angle is 2°,the resuls show the central part of the weld zone is observed to be dynamically recrystallized The structure of 2024 aluminum alloy shown as recrystallized equiaxed grain and represents some static grain growth after welding. The grain size is much smaller near the weld bottom, Overall, the weld zone exhibited an equiaxed grain structure roughly one-tenth the average base metal grain size. It can be noted in the figure 2.5 that a rather large ‘tunnel’ of unwelded material exists near the weld bottom resulting by a slightly fore shortened tool. Also there is a 1 mm section at the bottom was not affected by the rotating tool. The FSW of 2024 Al to 6061 Al produces intercalated flow microstructures consisting of dynamically recrystallized grains which facilitate superplastic stirring of one metal into the other. These equiaxed, dynamically recrystallized grains are observed to grow by 10 to 100 times the original

recrystallized grain size. There was no difference in the lamellar regions between 2024 Al and 6061 Al. The regions were observed to etch differently and produced sharp contrast features in optical metallography. This provided clearly images illustrating flow visualization and complex flow patterns which were observed to vary with tool rotation speeds, increasing tool rotation speeds produced slightly larger equiaxed residual grain structures, and at tool speeds in excess of 800 rpm dislocation spiral networks were observed in the 2024 Al lamellae. The weld strength was observed to fluctuate across the weld zone and reach a minimum within the 6061 Al near the FSW zone transition region where the actual, residual microhardness decreased by as much as 40% from the un-welded, 6061 Al workpiece microhardness. Although a good quality, contiguous weld can be achieved in the 2024 Al. Figure 2.5 show the Al2024 and Al6061 FSW microstructure weld cross-section.

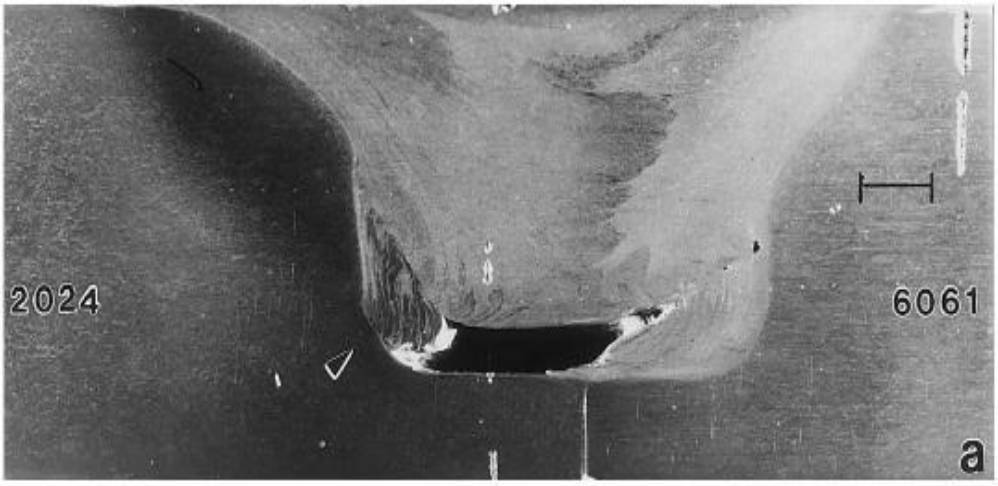

Figure 2.5 Representative Al2024 and Al6061 FSW microstructure weld cross-section showing large tunnel and unwelded plate at weld bottom (Ying Li. et.al. 1999)

J.H. Ouyang and R. Kovacevic (2001) studied the material flow and microstructural evolution in the friction stir welds of a 6061-Al alloy to itself and of a 6061-Al alloy to 2024-Al alloy plates of 12.7 mm thickness, The rotational speeds used was 151-914 rpm with a travel speeds of 57-330 mm/min for. The results showed asymmetry characteristics of plastic deformation, flow, and mechanical mixing of the material at both sides of the same and dissimilar welds. The microstructure show an alternative lamellae with different alloy constituents for a weld of 6061-Al to 2024-Al alloy, are attributed to the stirring action of the tool. The mixing in the dissimilar metal welds is incomplete instead of the complete bonding between the alloys. In summary, observations showed that FSW parameters especially the rotational and traverse speed have the significant effect on the mechanical properties and the residual microstructures and controlling these operational variables increasing the weld efficiency.

CHAPTER 3

EXPERIMENTAL WORK

3.1 Introduction

This chapter highlights on the standard procedures and techniques that are used to prepare materials for welding by friction stir technique, process parameters used, machining operations and the mechanical testing to evaluate the mechanical behavior of the welded joints. This is beside to the evaluation of microstructural changes of the weld area.

3.2 Material used

Dissimilar 2024-T3 and 6061-T6 aluminum alloys of 3 mm thick plates were friction stir butt welded. AA2024 is an aluminum alloy with copper Al-Cu of the 2xxx series with a temper condition of solution heat treated, cold worked, and naturally aged. It is usually used where good machinability and high strength are required such as aircraft structures, especially wing and fuselage structures under tension. AA6061 is a precipitation hardening aluminum alloy, containing magnesium and silicon as its major alloying elements. Al-Mg-Si grade alloy of the 6xxx series of medium strength and extremely employed for welded engineering structural components and military application such as bridges, railway coach bodies, floor assembly, and structural truck components it is with a temper condition of solution heat treated and artificially aged.

The chemical composition of the base metals was tested by spectrometer device in the laboratory and engineering testing department of S.I.E.R (see Appendix A) and analyzed according to ASTM standard as illustrated in table 3.1. Also the mechanical properties of the base metals are presented in table 3.2.

Table 3.1 Chemical composition of the base metals (element concentration %).

Element	**AA2024**	**AA6061**
Si	0.1255	0.673
Fe	0.272	0.590
Cu	4.19	0.326
Mn	0.6144	0.066
Mg	1.26	1.03
Cr	0.012	0.196
Ni	0.010	0.013
Zn	0.165	0.108
Ti	0.018	0.015
Pb	0.0099	0.009
Al	93.4	96.9

Table 3.2 Mechanical properties of the base metals.

Material	Yield strength MPa	Ultimate tensile strength (UTS) MPa	Percentage of elongation %
2024-T3	380	464	16
6061-T6	295	342	10

Aluminum alloys AA2024 and AA6061 with a thickness of 3 mm was cut to 100 mm width and 200 mm in length, the cutting process was followed by machining the edges for the desired dimensions for the purpose of excellent assembly.

3.3 Friction stir welding tool

The FSW tool has been fabricated from a high speed steel (HSS). Figure 3.1 (a) shows a close-up view of the tool that has been used in making all weld trials. The tool has a concaved shoulder of 18mm diameter, while the tool pin has cylindrical shape. The diameter of the pin is 6mm with an overall height of 2.8 mm making it slightly shorter than the plate thickness. Figure 3.1 (b) shows the dimensions of the tool used in the current study. This tool geometry has been obtained by many of the initial welding trials.

Figure 3.1 (a) FSW tool used in the current study

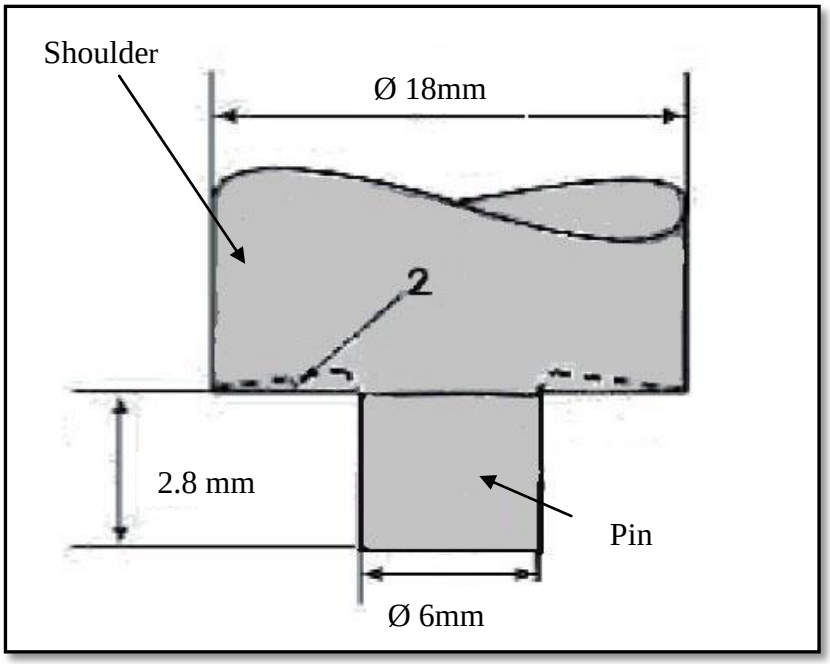

Figure 3.1 (b) Schematic of FSW tool used in the current study

3.4 Friction stir welding operation

In the first the welding experiments were carried out using a CNC-controlled milling machine shown in Figure 3.2

Figure 3.2 The milling machine utilized for friction stir welding (FANUC Series 21-MB)

Using a 0˚ tilt angle and after several trials, the weld performance was not successful because of the presence of tunnel visual to the surface portion and also it was indicating by the incomplete circle of the hole at the end of the weld line, therefore, a 1˚ tilt angle used by rotating the head of the milling machine using the scale available in the machine with the aid of using digital scale also which provide a successful weld as it is shown in figure 3.3.

Figure 3.3 The digital scale used for rotating the head of the vertical milling machine to satisfy the required tilt angle

As the CNC machine used was 3dimentional movement i.e. the option of rotating was not available, another vertical machine was used which provide the previous option as shown in figure 3.4. The welding parts are put on backing plate was in turn fastened into the milling machine table. Then supporting them using specially designed mechanical clamps as shown in figure 3.4 which illustrates the overall geometry of this process. The abutted surfaces were only fine machined with a milling machine to remove surface oxides.

The plates were tightly clamped with rolling directions aligned next to each other. The rotating tool pin was slowly pushed into the seam axially until the tool shoulder came into contact with the surface of the material, which generated frictional heat to locally soften the material around the pin. The penetration depth of the tool shoulder into the plates was about 0.2 mm, and the axial position of the pin tool was held constant while it traversed along the seam at a constant speed.

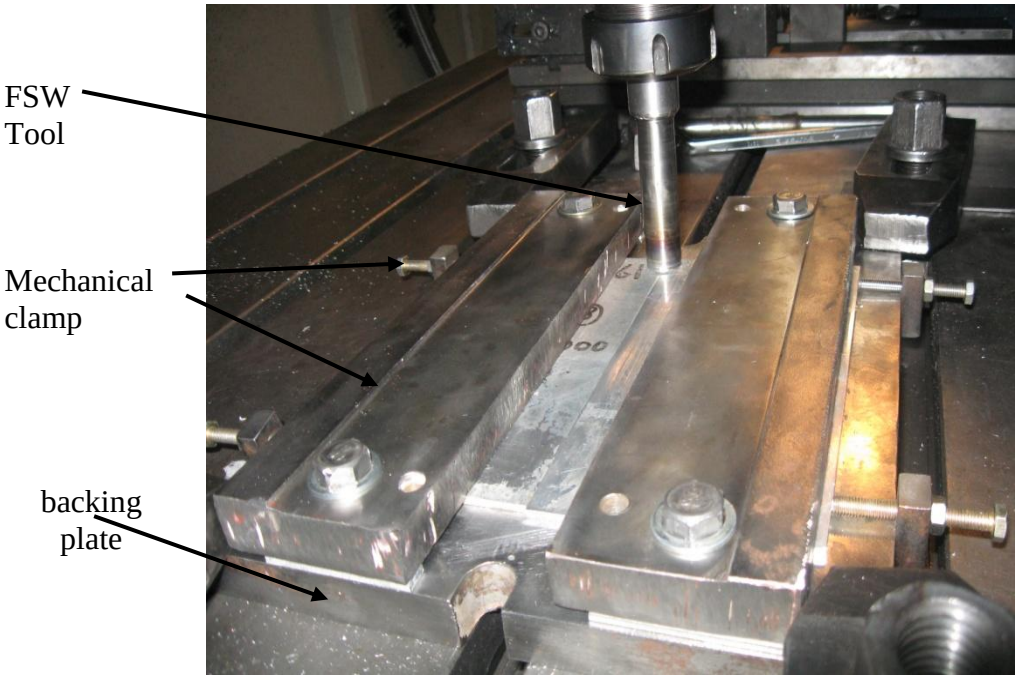

Figure 3.4 A close-up view of friction stir butt welding

Square butt joint configuration has been prepared by cutting and milling the edges and cleaning the abutted surfaces to fabricate friction stir welded joints as shown in figure 3.5. The parts to be welded should abutted hardly by adjusting them using the designed clamps.

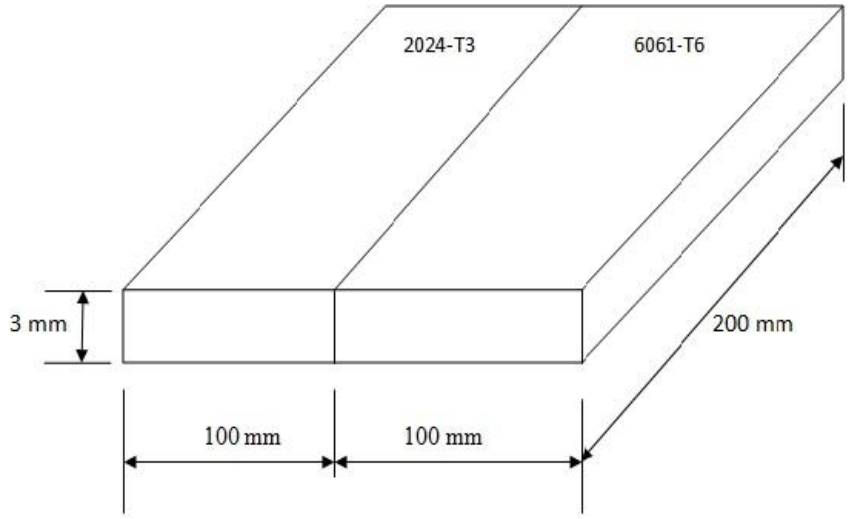

Figure 3.5 Shape and size of the square butt joints used in the current work

During welding, the tool was rotating in the clock-wise direction and was tilting 1°degree with respect to the vertical axis in order to maintain more pressure on the plasticized material behind the tool to produce quality welds. The downward pressure *P* of the tool is kept constant throughout the experiments by keeping the plunging depth of the rear of the tool shoulder at about 0.2mm. The time taken by the tool to completely penetrate into the butt interface (plunging rate) depends on the hardness of the base metal and tool rotational speed. The welding parameters used to fabricate the joints are presented in table 3.3 and table 3.4. Too many of initial welds were fabricated in order to examine the ability to produce the same quality of the welds under the same conditions. A total of 20 joints were fabricated using different combinations of tool rotational speed, tool travel speed in order to reach the final successful joints.

Table 3.3 Friction stir welding process parameters used to fabricate the joints.

Sample number	Transverse speed mm/min	Rotation speed rpm	Direction of weld
1	50	600	2024 0n advanced side & 6061 on retreating side
2		800	
3		1000	
4		1200	
5	50	600	6061 0n advanced side & 2024 on retreating side
6		800	
7		1000	
8		1200	

Table 3.4 Second process parameters used to fabricate the joints

Sample number	Rotation speed rpm	Transverse speed mm/min	Direction of weld
9	1000	25	6061 0n advanced side & 2024 on retreating side
10		75	
11		100	

3.5 X-Ray radiographic test

The first step in characterizing the welds was a visual inspection and qualitative analysis of the weld roots and crowns. X-ray inspections test of welded specimens were also carried out to check that no defects like root flaws or kissing bond were present in the welds. using Radiographic unit operated at 150 kV, 2 mA and duration

of 1 min. To determine the quality of the weldment for pores and discontinuities at weld nugget.

3.6 Tensile test

Tensile properties of each joint were evaluated at room temperature using the computerized Tinus Olsen universal tensile testing machine shown in figure 3.6. All tensile tests were carried out at a constant crosshead speed of 10mm/min and the average of three specimens was taken to evaluate the tensile behavior of each welded joint. The elongation was measured using the formula of:

$$\%EL = \frac{Lf - Lo}{Lo} \times 100 \qquad \text{(William D. Callister, 2001)}$$

where Lf: is the fracture length after testing and L_0 is the original gage length.

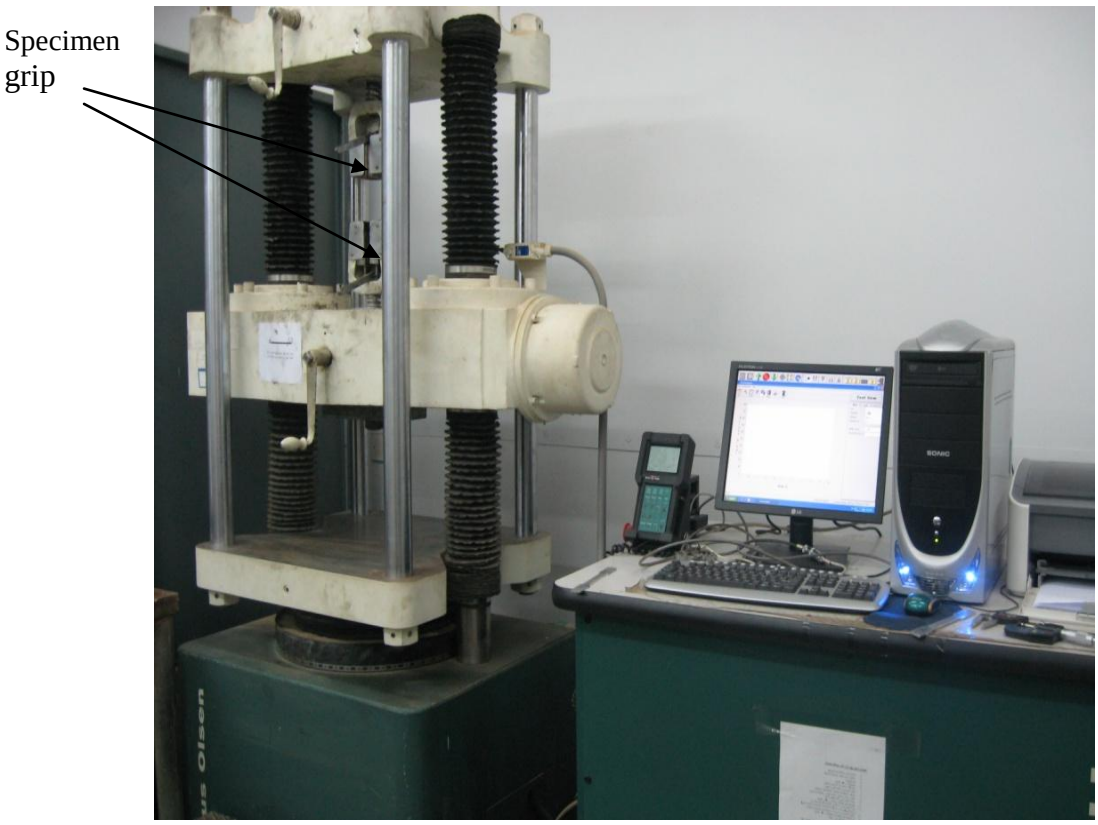

Figure 3.6 Tinus Olsen universal tensile testing machine in Central Organization for Standardization & Quality Control.

Tensile testing was carried out perpendicular to the welding direction to determine the tensile properties of the welded joints. The configuration and dimension of the transverse tensile specimens was taken according to ASTM (E8M-04) as it is shown in figure 3.7.

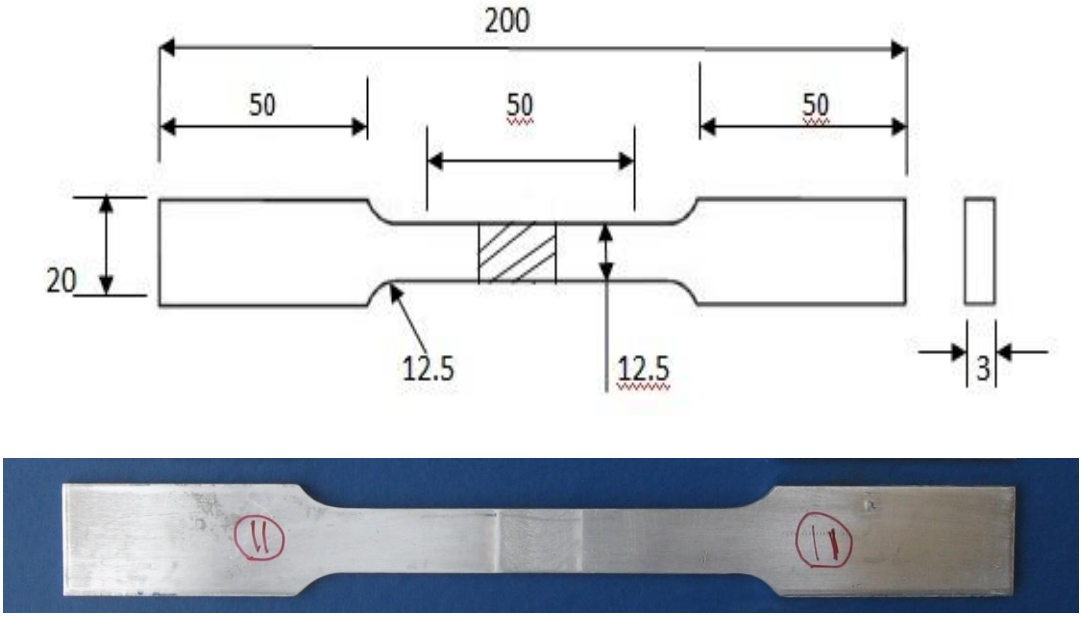

Figure 3.7 Tension test specimen geometry, dimensions are in millimeters

3.7 Bending test

The machine used in the testing was a universal electro-mechanical tensile and bend testing machine as it is illustrated in figure 3.8. The welded joints were machined into standard test specimen dimensions according to the ASTM (E 190-92) as it is shown in the figure 3.9. The diameter of the former was (24 mm) depending on the diameter factor of the material according to ASTM 209, which is equal to N times the thickness of the plate. Face and root bending tests were carried out at room temperature by universal testing machine for the purpose of evaluate the bending properties and ductility which is considered as an important mechanical property to measure the degree of plastic deformation that has been sustained at fracture.

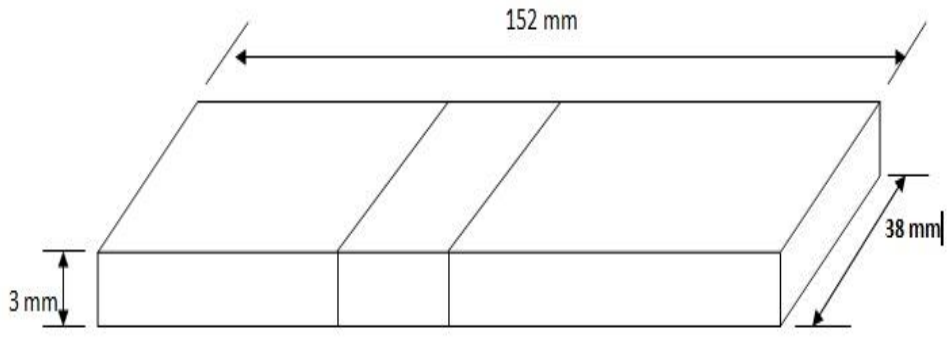

Figure 3.8 Schematic of bending test specimen according to ASTM (E 190-92)

Figure 3.9 Bending device

3.8 Microhardness testing

Microhardness testing of the welded joints was published using the Vickers hardness tester shown in figure 3.10. Vickers hardness measurements were taken 1mm below the top surface of the specimen's perpendicular to the welding direction using a diamond pyramid indentor with a load of 20Kg and loading within 15sec. The fabricated joints were cut into suitable pieces and then the pieces were machined to the required size to prepare specimen for mechanical testing and microstructural examination. The surface of the specimens was prepared using different grades of emery papers to remove machining marks and provide a suitable flat surface. Vickers hardness profile will indicate to the microstructural changes had taken place due to the thermal cycle of the friction stir welding operation.

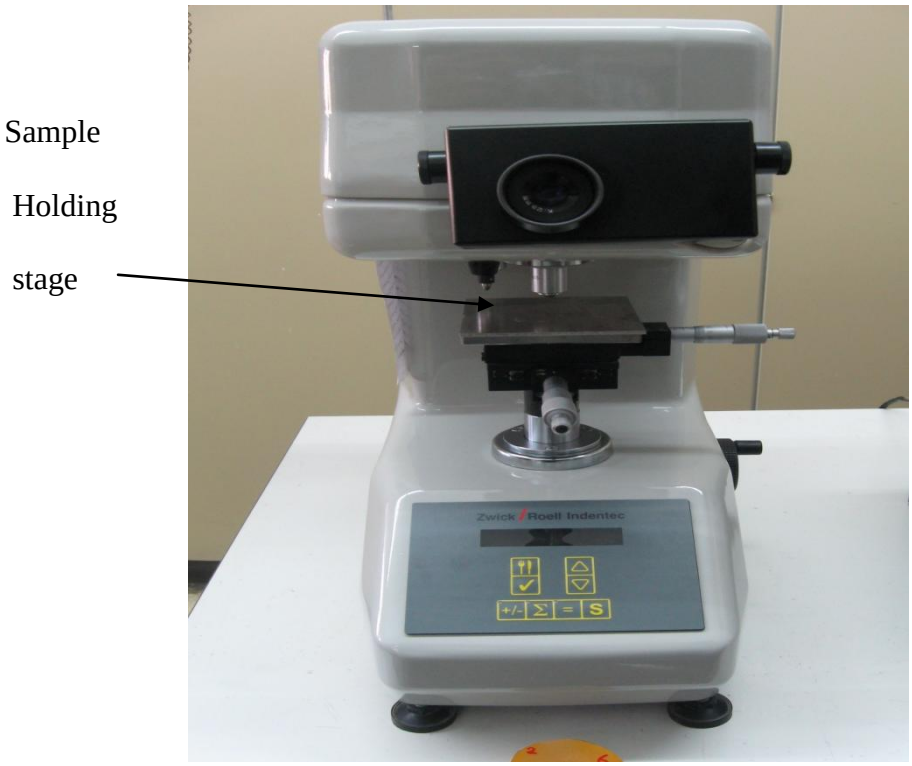

Figure 3.10 (a) Zwick/Roell microhardness digital tester.

Figure 3.10 (b) Clause-up view for the holding stage and indenter.

3.9 Microstructural evaluation of the weld area

The macro and microstructural features of the friction stir welded joints were investigated using a union optical metallurgical microscope of the type shown in figure 3.11 equipped with a 3 mega-pixel eyepiece digital camera and connected to a PC via a USB port driven by an image-capture software system. The specimens for metallographic examination were cut using the handsaw to the required sizes from the joint containing the nugget zone (NZ), the thermomechanical affected zone (TMAZ), the heat affected zone (HAZ), and the base metal (BM) for the both alloys as it is shown in figure 3.10. According to the ASTM E3 the specimens mounted by a polymeric material to protect them from damage and to provide a uniform format for the manual preparation. Using the castable plastic method the preparation done in room temperature using resins consist of two components (self-curing denture base acrylic resin) mixing together and wait for 8-15 min for the cure time. The specimens are then prepared through a series of successive steps starting from grinding (rough and fine stages) using different grades of emery papers (120, 240, 320, 400, 600, 800, 1000,1200 and 2000) with a lubricant material for the purpose

of removing sectioning damages and substantial amounts of specimen material and also for level the mount surface , the specimens rotated at 45-90degree, polishing on the disc polishing machine to a mirror finish using AL_2O_3 with a soft cloth and two successive grades of diamond compound suspension; a coarse compound of 1μm particle size followed by finer compound of 0.25μm particle size. and finally etching in special chemical solutions.

The polished sections were then washed in warm water and dried in a furnace blowing hot air. Etching of the prepared sections was done using Keller's reagent (2ml concentrated hydrofluoric acid HF, 3ml concentrated hydrochloric acid HCl, 5ml concentrated nitric acid HNO_3, and 190ml distilled water H_2O) to reveal microstructural features of the different zones of the friction stir welded joints. Observations of plastic deformation, material flow, and microstructures are performed by using a high-resolution optical microscope.

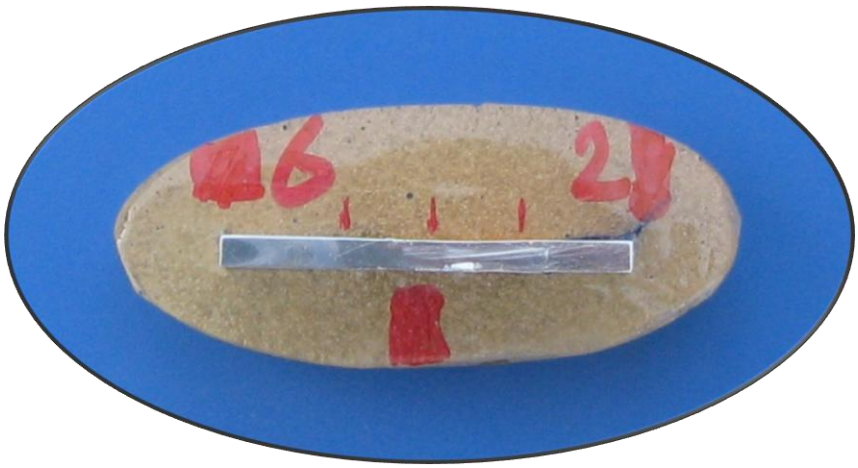

Figure 3.10 The specimen of microstructure testing

Figure 3.11 Optical microscope equipped with an eyepiece digital camera.

CHAPTER 4

RESULTS AND DISCUSSION

4.1 Introduction

In this chapter, the laboratory results for microstructure and mechanical properties for the friction stir welded dissimilar aluminum joints of 2024-T3 and 6061-T6 were studied. The thermomechanical process which include generations of frictional heat coupled with sever plastic deformation during friction stir welding in the weld area, results in metallurgical transformations and degradation of mechanical properties of the base alloy. The amount of heat generated and the associated plastic deformation and material flow are all affected by many of the process parameters, such as tool rotation and travel speeds, tool design and the base alloy mechanical properties and thermal history. For the present study, a single tool of a constant design and constant tilt angle has been used to fabricate all the weld trails and therefore the effect of the tool design will be eliminated. Welding conditions will involve tool rotational speed, tool travel speed, tilt angle and location of the alloys with respect to the welding direction.

4.2 Effect of tilt angle on the joints fabricated by friction stir welding

The use of 0˚ tilt angle lead to unsuccessful weld performance due to the presence of tunnel running along the weld line and it was indicating by the incomplete circle of the exit hole at the end of the weld line as it is illustrated in figure 4.1, while, using a 1˚ tilt angle provide a good weld without any tunnels.

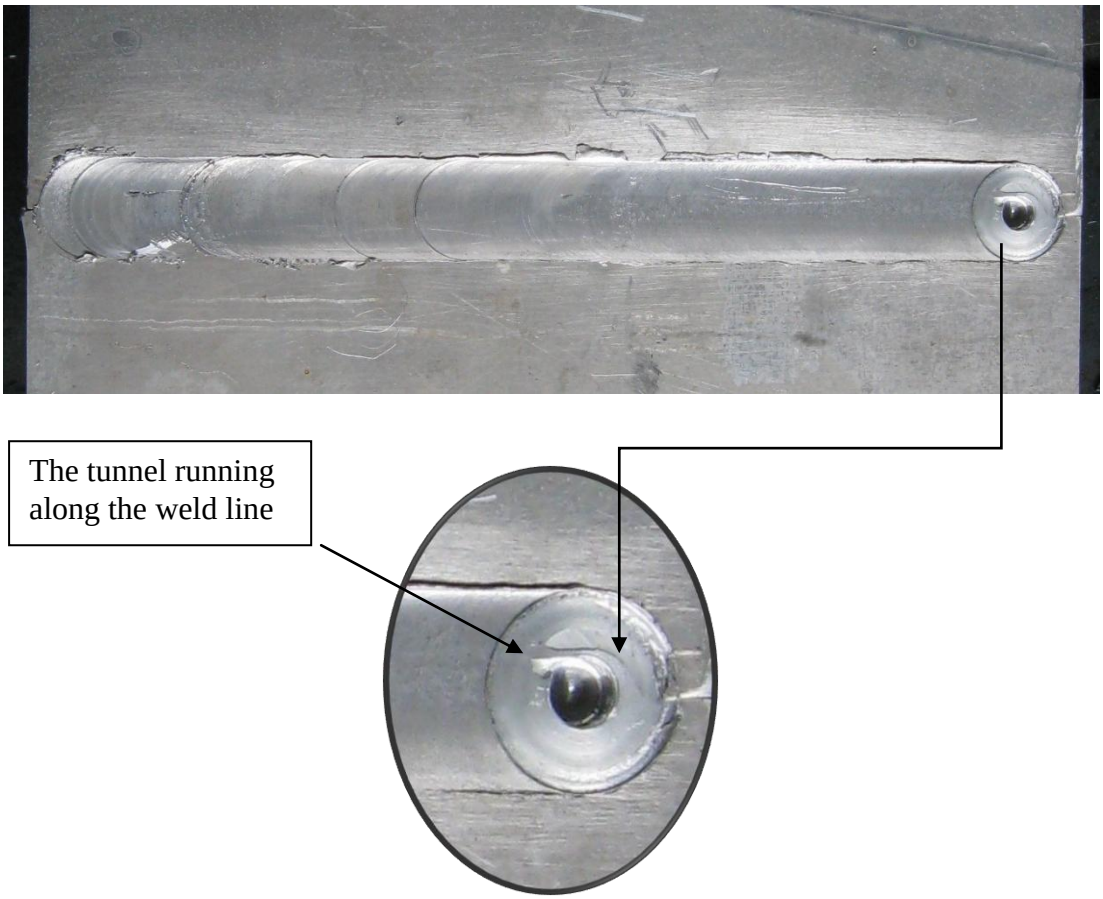

Figure 4.1 The appearance of the welds using 0˚ tilt angle

4.3 Effect of rotational and travel speeds on the appearance of the weld

Figure 4.2 show the weld surface appearance made with the cylindrical pin profile at different rotational speed (600, 800, 1000, 1200 rpm). The weldments indicated no visible defects, weld surface is even and uniform. It can be seen from the pictures that better surface appearance has been obtained at these rotational speeds.

At higher rotational speed of 1200rpm, plastic deformation is more produced due to increasing in the heat generation which can flow to the surrounding of the material. There were no irregularities on both the face and root. Also the exit hole at the end of the weld was examined. A circle of material that is deformed by the tool shoulder always remains at the end of the weld. The appearance of this circle provides information about the weld quality. With a good weld the circle around the exit hole

is 100% complete. In all the joints of this work there was a flash extending from the beginning to the end of the weld.

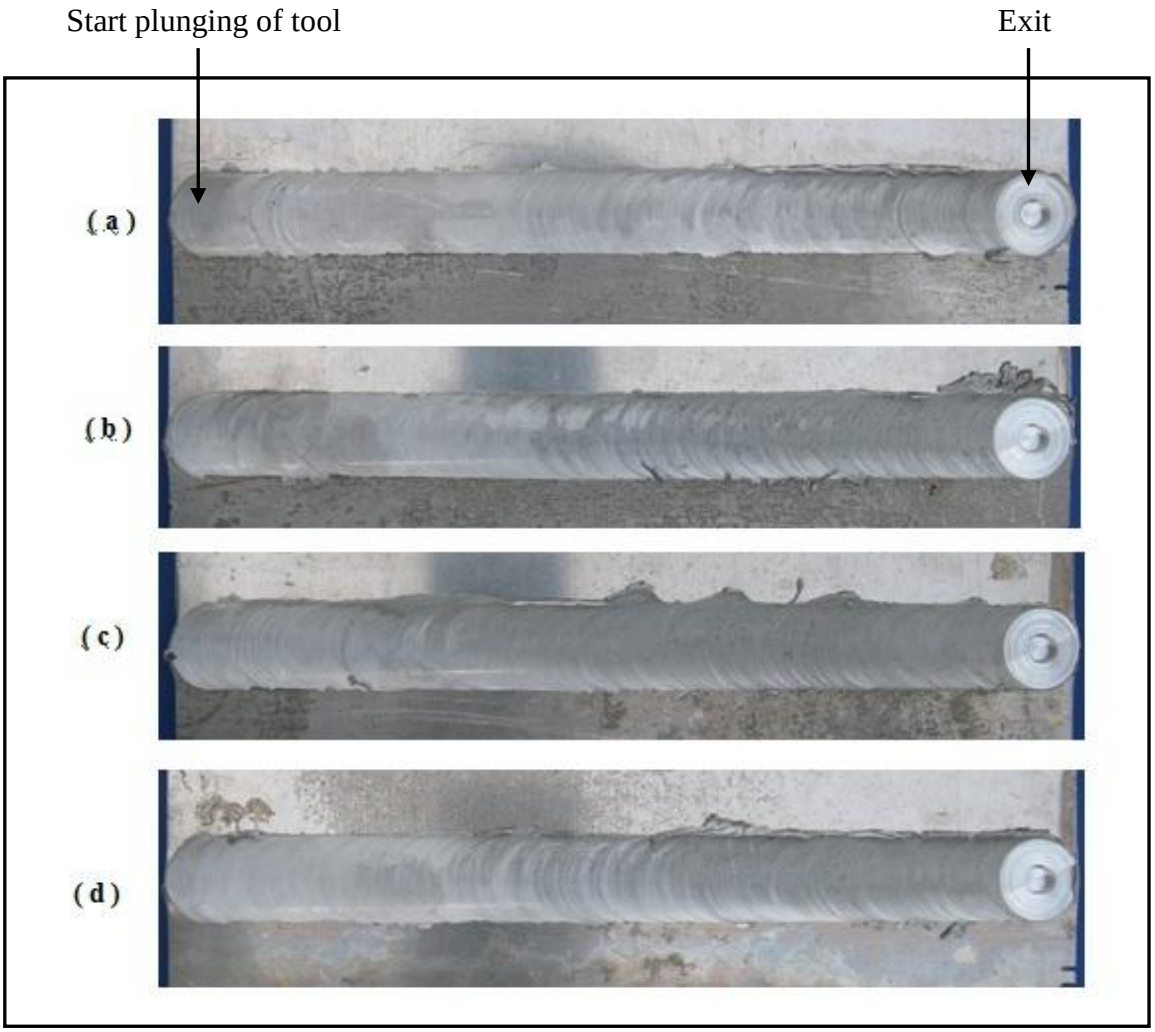

Figure 4.2 Appearance of the weld using cylindrical pin and variable rotation speed of: (a) 600rpm, (b) 800rpm, (c) 1000rpm and (d) 1200rpm at traverse speed of 50mm/min

It can be seen that there was no differences between the weld surface appearance of the weldments when locating the aluminum alloy 2024-T3 on advancing side and 6061-T6 on retreating side or vice versa. Figure 4.3 show the weld surface appearance of the third group of welding using variable traverse speed of (25, 75, 100 mm/min) and keep the rotational speed constant. It can be seen that high traverse speed result a smooth surface appearance.

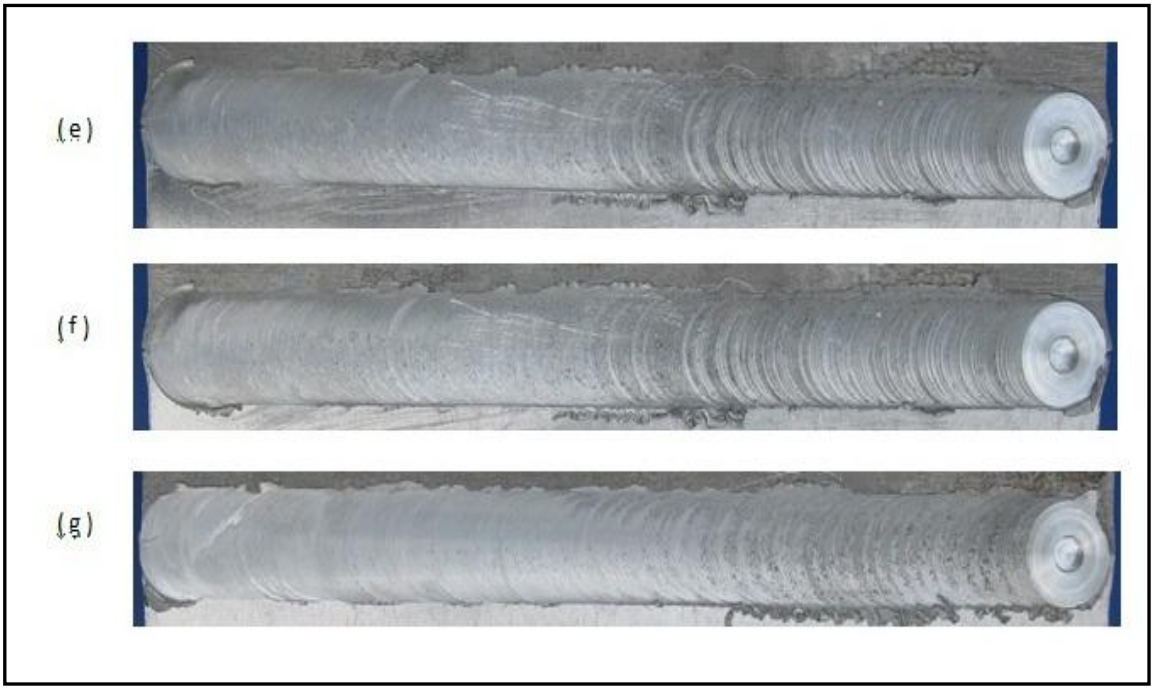

Figure 4.3 Appearance of the weld using cylindrical pin and variable traverse speed of: (e) 25mm/min, (f) 75mm/min, (g) 100mm/min at rotational speed of 1000rpm

4.4 Radiography inspection

X-Ray radiographic inspection was carried out using Radiographic unit and the radiographs indicated a good quality weld without any pores and discontinuities at weldment (see Appendix B). This confirms the presence of no defects at weld nugget irrespective to tool rotation speed. Figure 4.4 and 4.5 show the radiographic images of 1st and 2nd group.

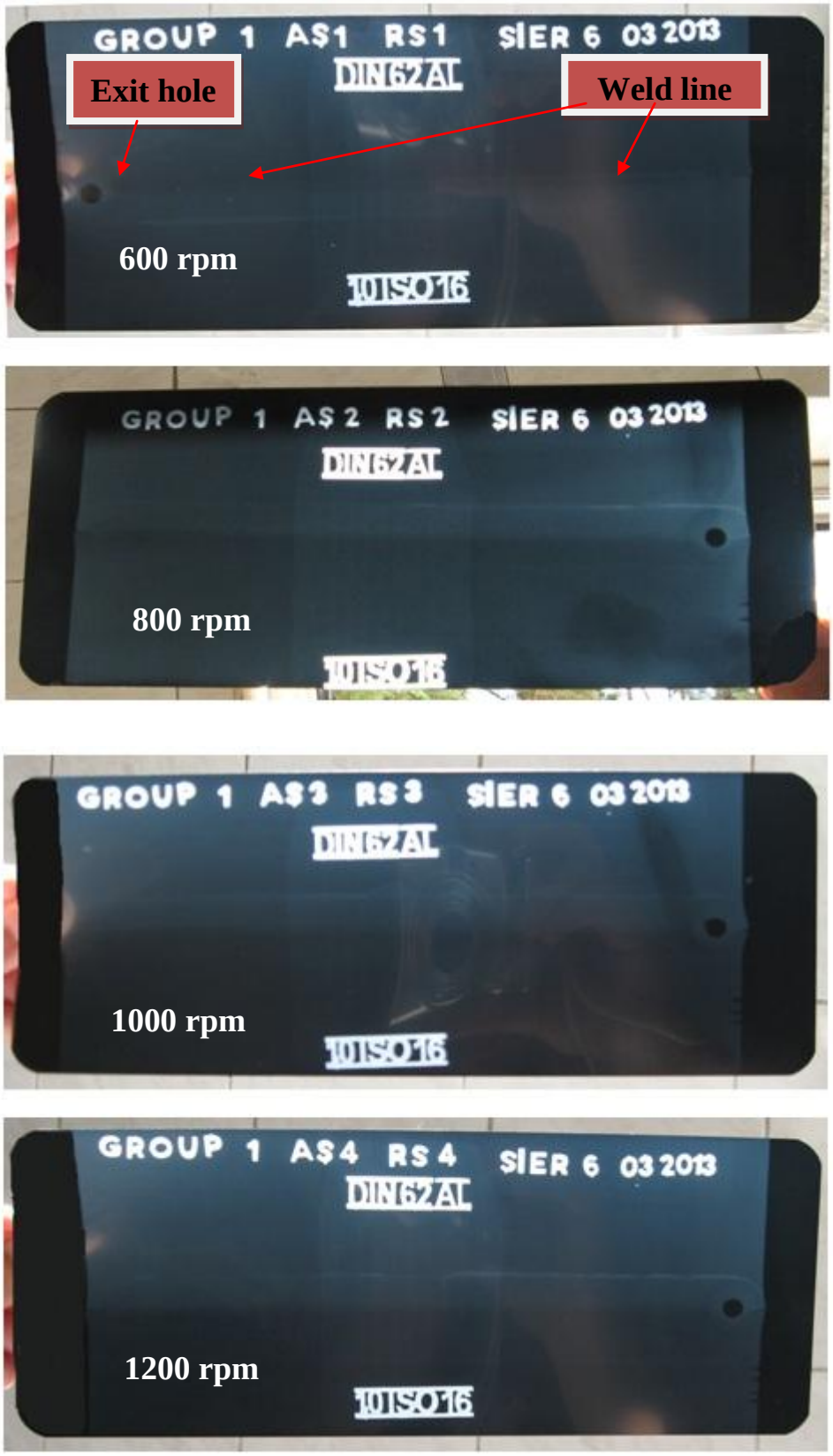

Figure 4.4 X-ray radiographic tests of the specimens for the case of locating aluminum alloy 2024 on advancing side

Figure 4.5 X-ray radiographic tests of the specimens for the case of locating aluminum alloy 6061 on advancing side

4.5 The effect of process parameters on tensile properties

Tensile properties such as tensile strength and percentage of elongation were evaluated for welded plates and compared with base metal. Table 4.1 shows the tensile properties of the base metal for both the aluminum alloys 2024-T3 and 6061-T6.

Table 4.1 Tensile test results of the base metals

Material	Yield strength MPa	Ultimate tensile strength (UTS) MPa	Percentage of elongation %
2024-T3	380	464	16
6061-T6	295	342	10

Also, the stress–strain curves obtained in the tensile tests of base materials 2024-T3 and 6016-T6 are plotted in Fig 4.6 (a) and (b).

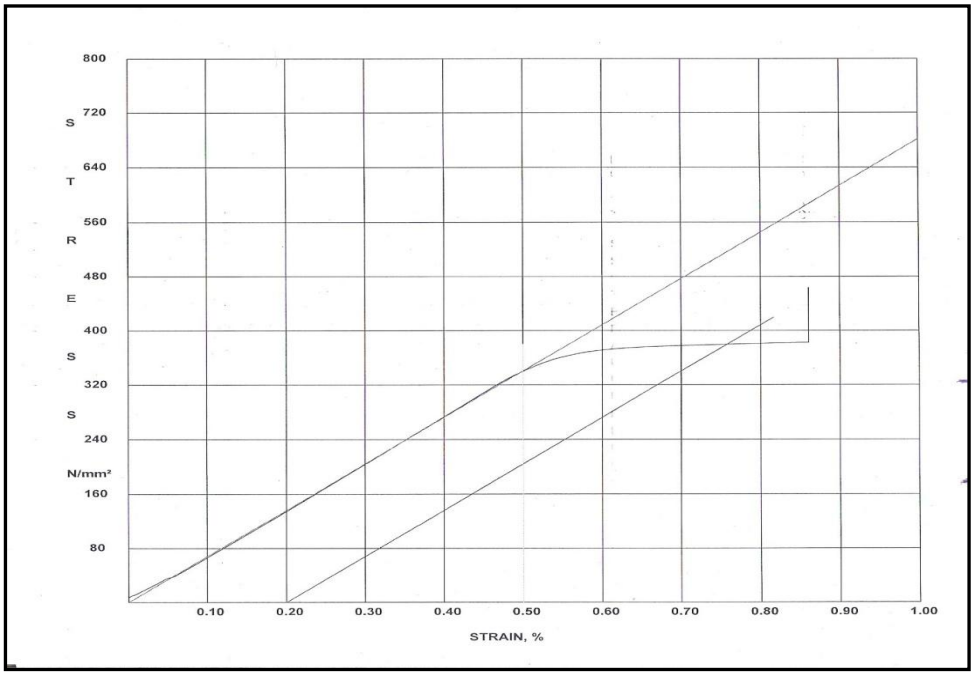

Figure 4.6 (a) Stress-strain curve of base metal AA2024-T3

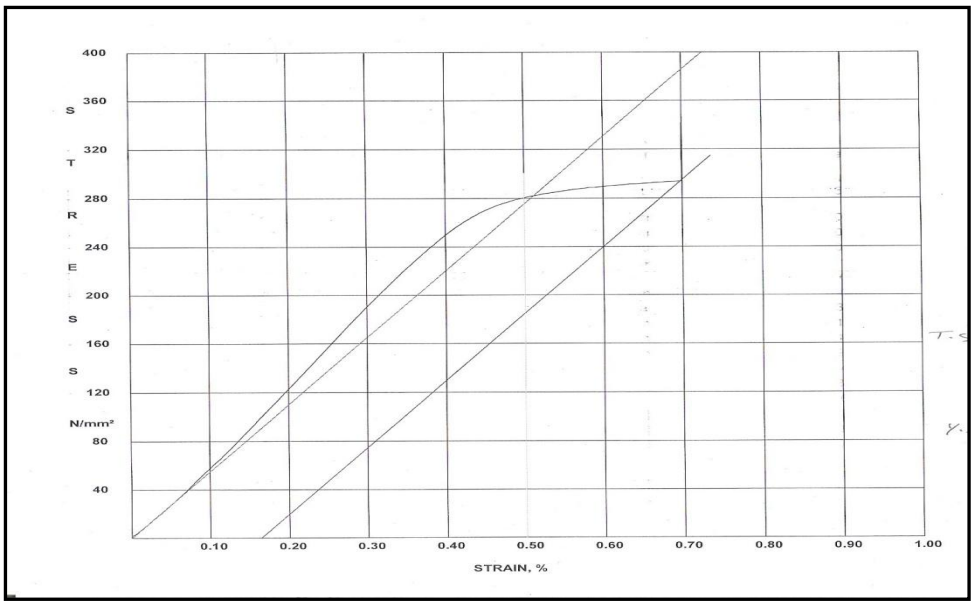

Figure 4.6 (b) Stress-strain curve of base metal AA6061-T6

Table 4.2 show the tensile test results of friction stir welded joints of dissimilar aluminum alloys 2024-T3 and 6061-T6 for the case of locating aluminum alloy 2024-T3 on advancing side.

Table 4.2 Tensile test results of the weldments for the case of (2024 at advanced side)

Traverse speed mm/min	Rotation speed rpm	AA 2024-T3 Located at advancing side				
		Yield Strength MPa	Tensile strength UTS MPa	Elongation %	Fracture location	Welding eff.%
50	600	165	195	7	At the NZ/TMAZ of 6061	57
	800	148	184	8	At the NZ/TMAZ of 6061	53
	1000	160	193	7.6	At the NZ/TMAZ of 6061	56
	1200	144	193	8.5	At the NZ/TMAZ of 6061	56

The yield strength and ultimate tensile strength of FSW joints are lower than the base metal. The highest value of the ultimate tensile strength recorded at rotational speed of 600 rpm and traverse speed of 50mm/min.

Stress–strain curve of the tensile tests for transverse weld sample of rotational speed 600 rpm and traverse speed 50 mm/min is shown in the figure 4.6 (c).

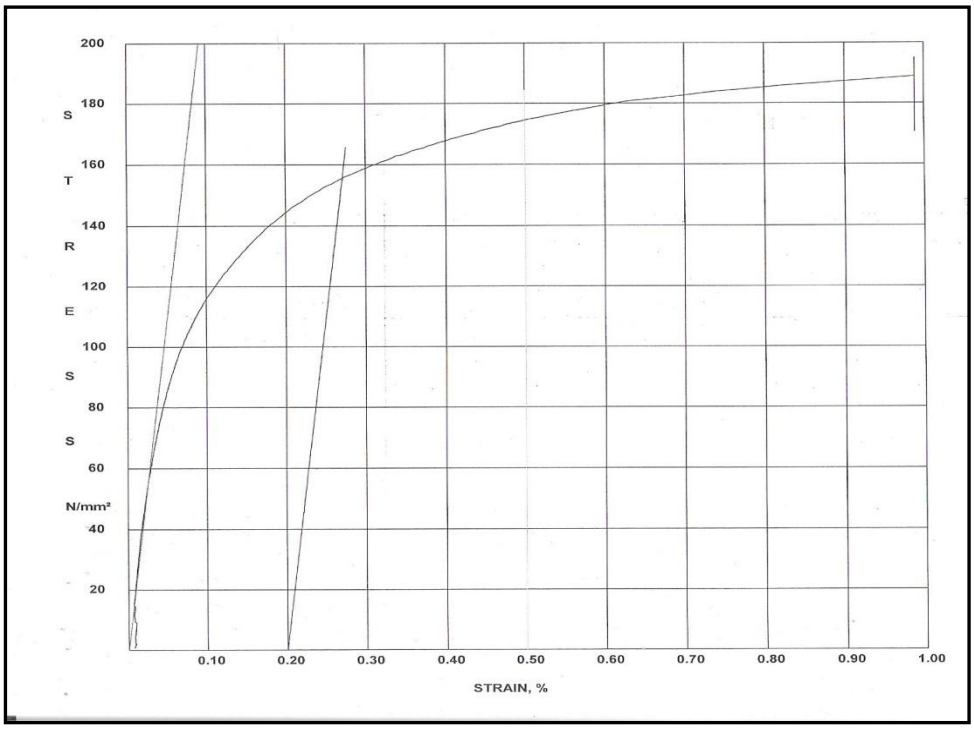

Figure 4.6 (c) Stress-strain curves for the case of AA 2024-T3 on advanced side using rotation speed 600 rpm

The fracture occurred in the SZ/TMAZ interface region of the 6061-T6 which was located on the retreating side as illustrated in figure 4.7.

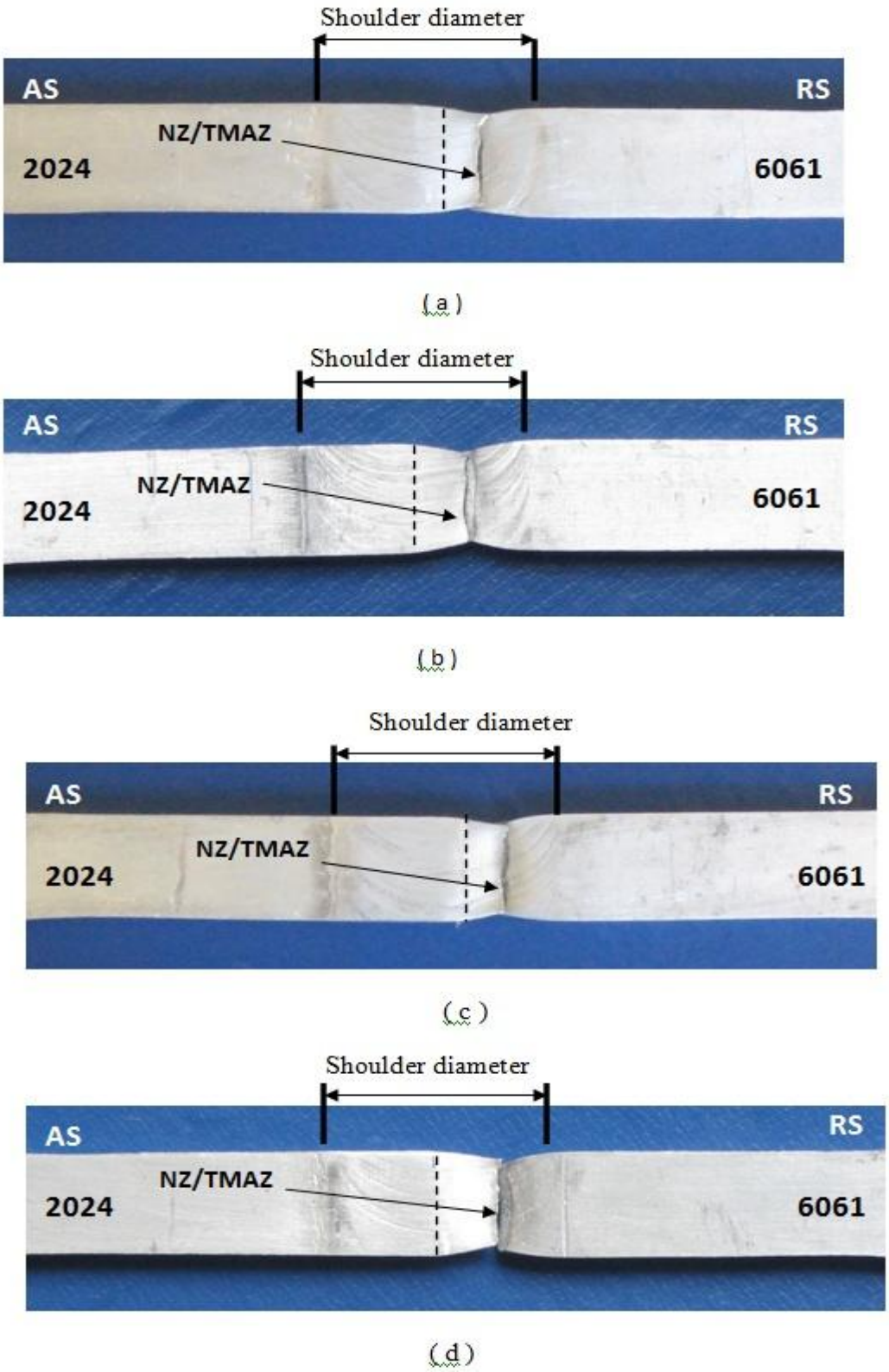

Figure 4.7 Fracture locations for the case of (2024 alloy on advanced side) at the rotational speed of (a) 600rpm, (b) 800rpm, (c) 1000rpm and (d) 1200rpm with a constant traverse speed of 50mm/min

Regarding the case of locating aluminum alloy 6061-T6 on advancing side, Table 4.3 present a better results than the first case, yield and ultimate tensile strength show a slight increase and the fracture occurred in the interface of TMAZ/HAZ region of the 6061-T6 alloy as it is shown in figure 4.9.

Table 4.3 Tensile test results of the weldments for the case of (6061 at advanced side)

Traverse speed mm/min	Rotation speed rpm	AA 6061-T6 Located at advancing side				
		Yield Strength MPa	Tensile strength UTS MPa	Elongation %	Fracture location	Welding eff.%
50	600	172	218	8	At TMAZ/HAZ of 6061	64
	800	176	212	6	At TMAZ/HAZ of 6061	62
	1000	179	220	8.8	At TMAZ/HAZ of 6061	64
	1200	176	215	7.5	At TMAZ/HAZ of 6061	63

The better condition was at rotational speed of 1000 rpm at travel speed of 50mm/min. Initially, the yield strength of the joints reached about 179MPa compared to 295MPa of the base alloy which accounts about 61% to that of the base alloy, while for the current case, the ultimate tensile strength reached values about 220MPa compared to 342MPa of the base alloy which accounts about 64% joint efficiency.

Stress–strain curve of the tensile test for transverse weld sample of rotational speed of 1000 rpm and traverse speed of 50 mm/min is shown in the figure 4.8.

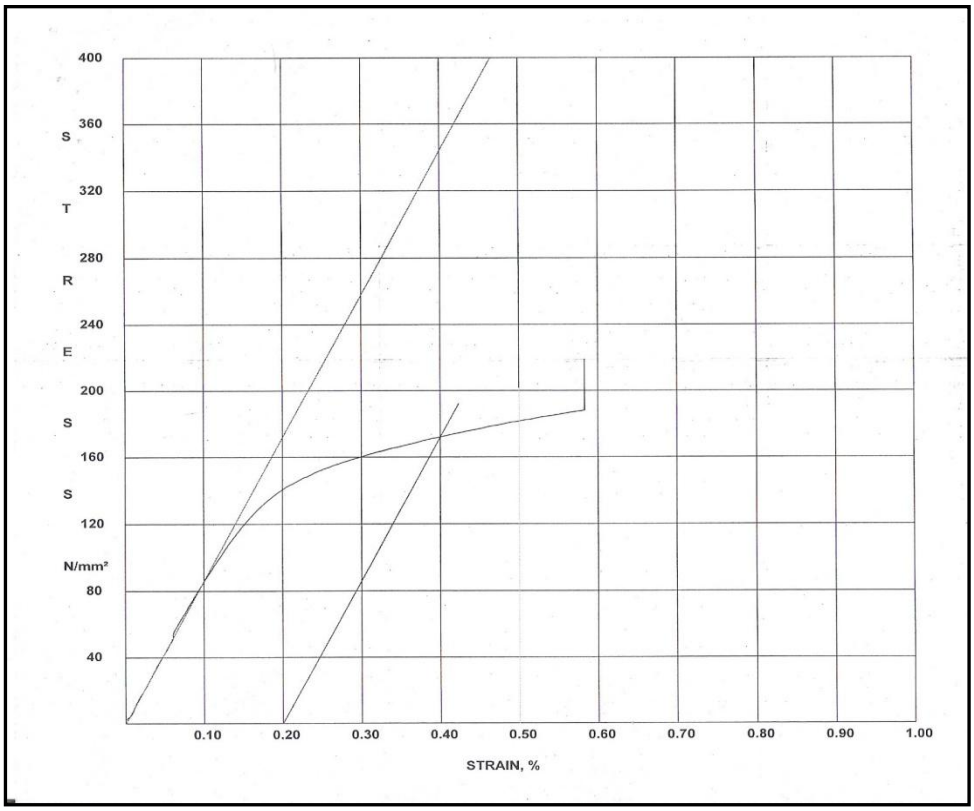

Figure 4.8 stress-strain curves for the case of AA 6061-T6 on advanced side using rotation speed 1000 rpm

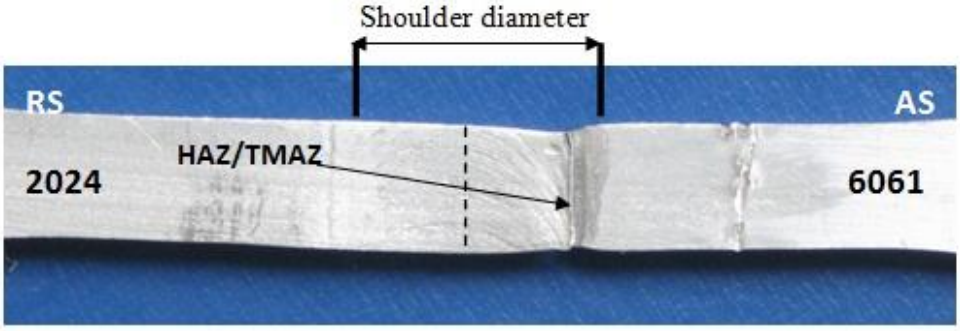

(e)

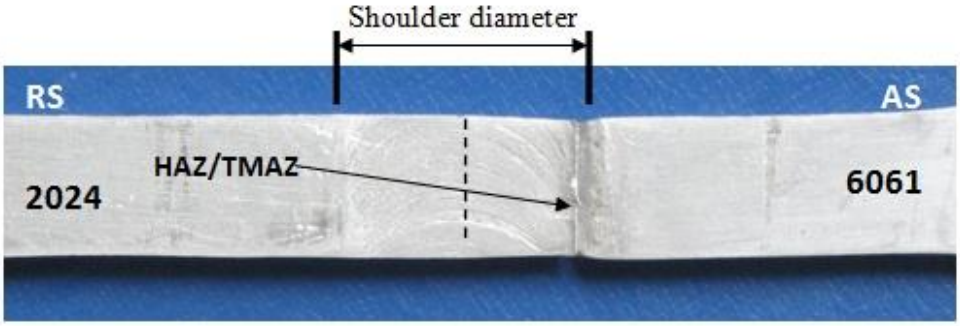

(f)

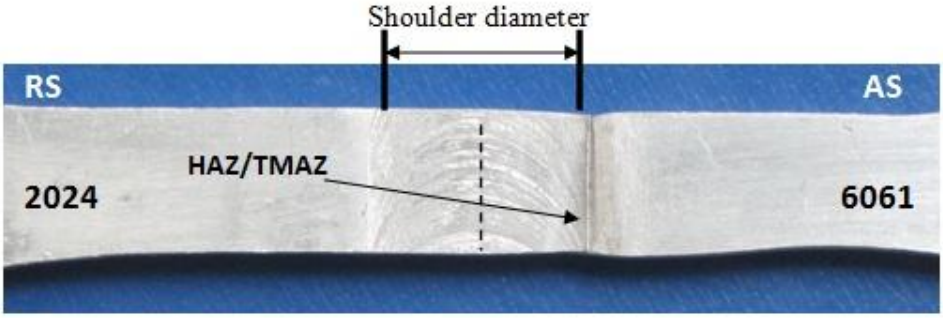

(g)

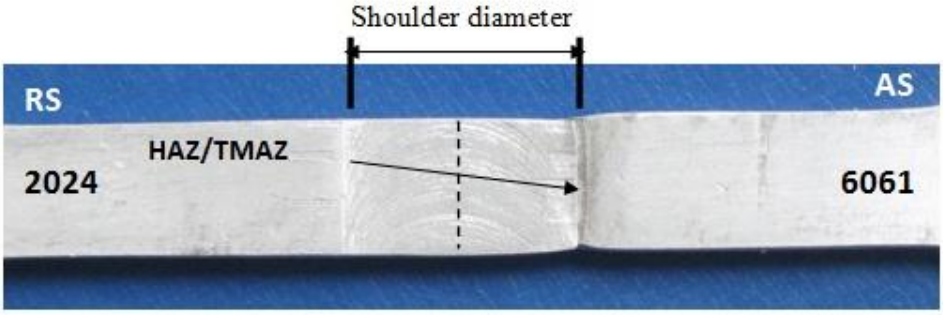

(h)

Figure 4.9 Fracture location for the case of (6061 alloy on advanced side) at the rotational speed of (e) 600rpm, (f) 800rpm, (g) 1000rpm and (h) 1200rpm with a constant traverse speed of 50mm/min

By keeping the location of the aluminum alloy 6061-T6 at the advancing side for the reason of providing better results , and using the better rotational speed of 1000 rpm with a new variable of traverse speeds (25 ,75 and 100 mm/min) as it is shown in the table 4.4. The yield strength and the ultimate tensile strength of the joints reached to a maximum value of about 154MPa and 206MPa respectively at traverse speed of 75 mm/min compared to 342MPa of the base alloy which accounts about 60% joint efficiency.

The fracture occurred in the TMAZ/HAZ interface region of the 6061-T6 which is considered as the weakest alloy due to its lower strength in compare with the 2024-T3 alloy as it is shown in figure 4.11.

Table 4.4 Tensile test results of the weldments for the case of (variable traverse speed)

Traverse speed mm/min	Rotation speed rpm	AA 6061-T6 Located at advancing side				
		Yield Strength MPa	Tensile strength UTS MPa	Elongation %	Fracture location	Welding eff.%
25	1000	144.5	190.3	6.1	At TMAZ/HAZ of 6061	56
75		154.2	206	4.4	At TMAZ/HAZ of 6061	60
100		150.7	206	4.3	At TMAZ/HAZ of 6061	60

Stress–strain curve of the tensile test for transverse weld sample of traverse speed of 75 mm/min at a rotational speed of 1000 rpm is shown in the figure 4.10.

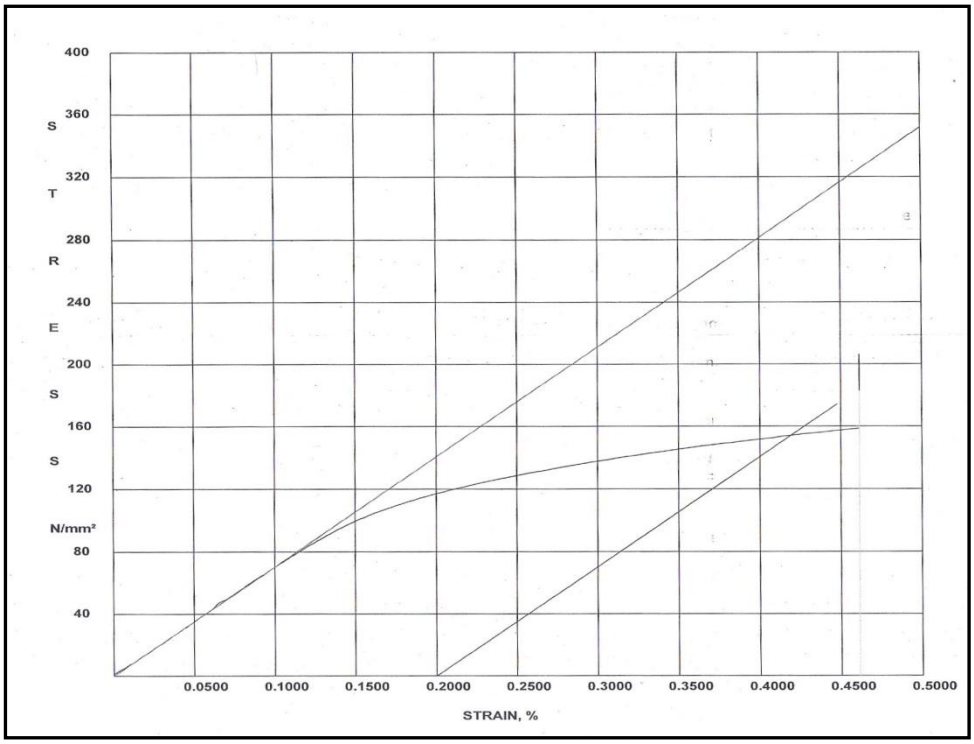

Figure 4.10 stress-strain curves for the case of AA 6061-T6 on advanced side and various travel speeds 75 mm/min)

Since the deformation is highly heterogeneous in the transverse weld samples, the stress and strain values plotted in the graphs are engineering values calculated from the initial geometry of the samples. The results reported in the graphs show that despite the yield stress values of weld samples are lower than the base material, the global ductility of the weld samples is smaller than the base material.

The decrease in ductility of the weld samples with respect to the parent metal is in accordance with previous results that reported severe hardness under match for the welds. Also, it can be associated with the cross-section variation along the specimens gauge length due to the thickness reduction in the weld. In fact, the engineering

stresses and strains for the samples were plotted considering a constant cross-section, 3 mm thick, along the entire gauge length of the samples.

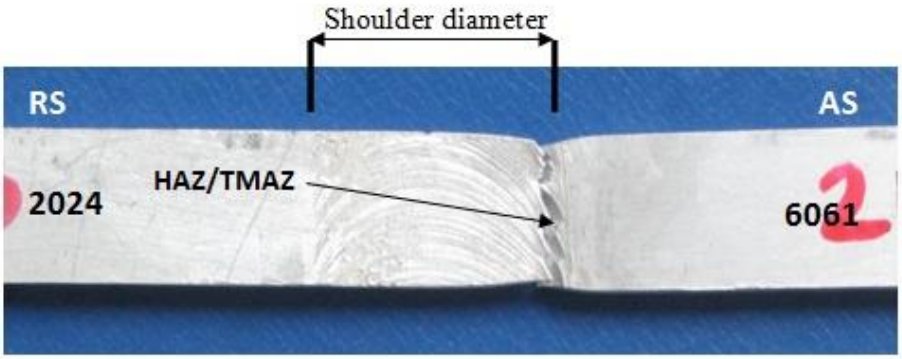

(i)

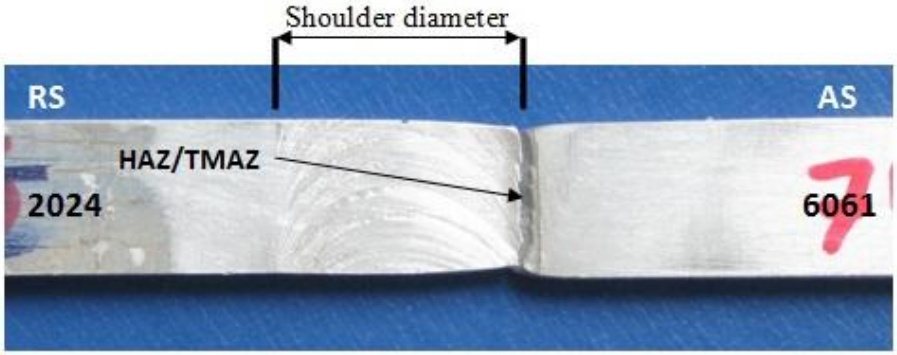

(j)

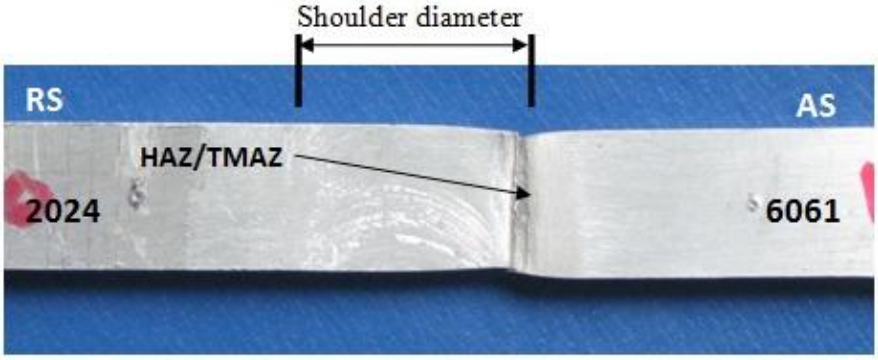

(k)

Figure 4.11 fracture location for the case of (variable traverse speed of (i) 25mm/min, (j) 75mm/min and (k) 100 mm/min at a constant rotation speed of 1000 rpm)

For the FSW joints of aluminum alloys, the fracture of the transverse tensile specimens occurred at the HAZ/TMAZ interface, i.e., the weakest zone of the joint. It is illustrated that all the tensile specimens failed roughly along the low hardness zones (LHZ), and the tensile strength of the welds corresponded well with the hardness values along the low hardness zones. This demonstrates that while the fracture location and inclination to the tensile axis of the FSW 6061-T6 joints were controlled by the position and inclination of the LHZs, the tensile strength was determined by the hardness values along the LHZs.

From the results shown in tables 4.2, 4.3 and 4.4, it is possible to conclude that the elongation of the best conditions of first, second and third case have, respectively, 88%, 80% and 61% lower ductility than the base material. The weld centerline for each of the specimens was marked. All of the welds exhibited the similar shear fracture pattern with a limited necking Figure 4.6. The shear fracture path was a ~45 to 60 degree angle to the tensile axis. The fracture position and fracture path correspond roughly with the low hardness zones (LHZ) .

The tensile properties of the dissimilar aluminum alloys 2024-T3 to 6061-T6 joint reveal four important findings. First, all the fracture locations occurs on the aluminum alloy 6061-T6 side due to the lower ultimate tensile strength with compare to the aluminum alloy 2024-T3, second, the better condition recorded at rotational speed of 1000 rpm at a constant traverse speed of 50 mm/min, third, the highest value of ultimate tensile strength (220 MPa) for the best condition was obtained by locating the aluminum alloy 6061-T6 on advancing side which is indicating that the retreating side has lower strength than the advancing side, Tensile properties of FSW butt joints of 2024-T3 plate and AA 6061-T6 plate depends mainly on welding defects and hardness of the joint. Fractures occurred at the Variation in tensile

strengths at different tool rotation speed was due to different material flow behavior and frictional heat generated. Also, material was pushed downward on the advancing side and moved toward the top at the retreating side within the pin. This indicates that the ‘‘stirring’’ of material occurred only at the top of the weld where the material transport was directly influenced by the rotating tool shoulder that moved material from the retreating side around the pin to the advancing side. Fourth, fracture location was at the TMAZ/HAZ interface.

4.6 The effect of process parameters on bending properties

Face and root-bend test was used as an important tool to understand about the ductility and toughness of the friction stir welds as it is illustrated in figure 4.12. In the case of forming defect-free joints, the bending angles of the joints are displayed in figure 4.13 a, 4.13 b and 4.13 c. In this figures it can be seen that with the change of the location of alloys (locating the aluminum alloy 6061-T6 on advancing side and 2024-T3 on retreating side), the bending angle increases gradually.

Both face bend and root bend tests were performed on the welded specimens of rotation speeds (600 , 800 , 100 and 1200 rpm) and for the travel speed of (25, 50, 75 and 100 mm/min). Most of the welds presented good bending properties and no cracks were observed. The first case with locating the aluminum alloy 2024 on the advancing side show a low ductility and bending properties and the bend location was at the side of 6061 aluminum alloy. These results were conducted in accordance with the tensile test results. The second case with locating the aluminum alloy 6061 on the advancing side have been result in good ductility which is reached to 8.8% at the rotational speed of 1000 rpm and 50mm/min and good bending properties which is showed a 180° bending angle (U shape) and no cracks were observed which indicated good quality weld with all rotating speeds.

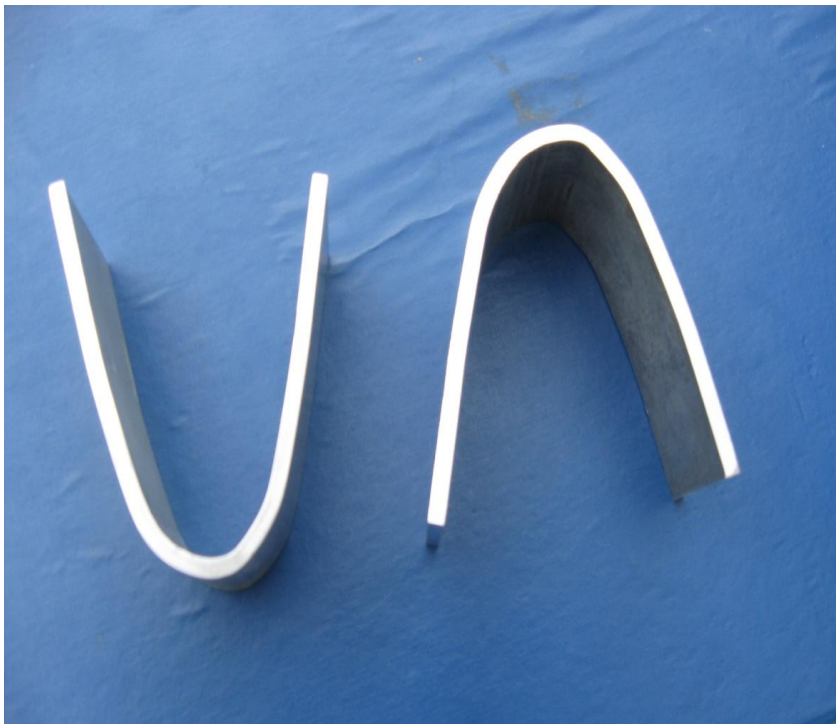

Figure 4.12 Face and root bending specimens

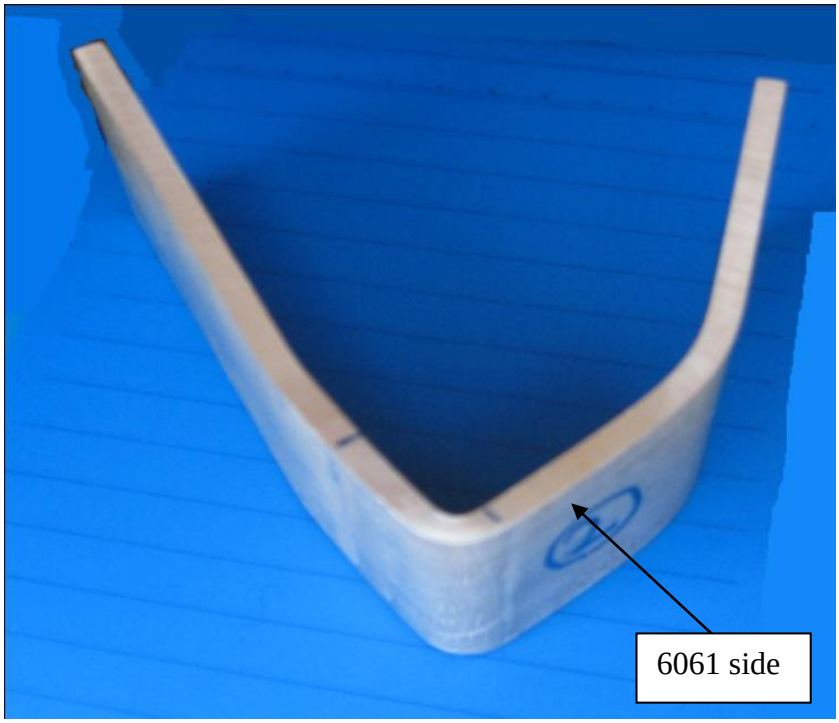

Figure 4.13 (a) Bending specimens for the case of 2024-T3 on advancing side

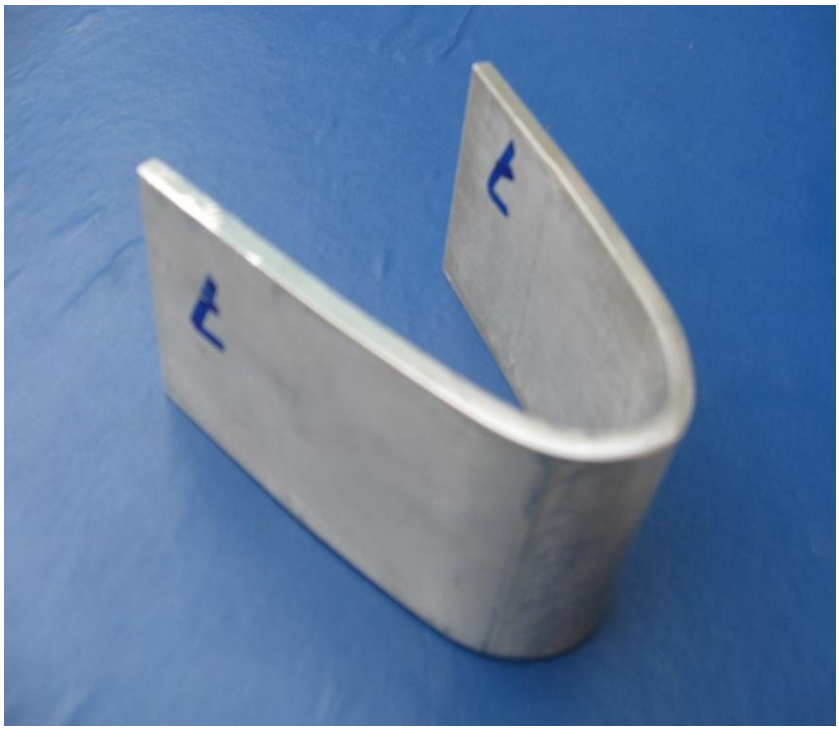

Figure 4.13 (b) Bending specimens for the case of 6061-T6 on advancing side

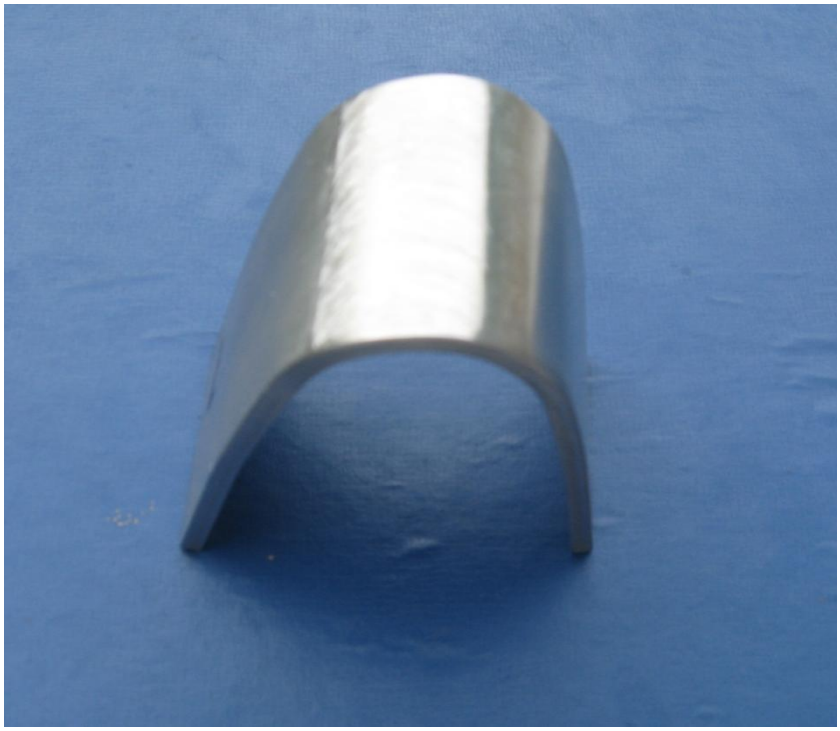

Figure 4.13 (c) Bending specimens for the case of using variable travel speed

4.7 Effect of welding conditions on microhardness profile of the weld area

Based on the tensile and bending test results of the previous section, it has been decided that the case with alloy 6061 on advancing side (with better mechanical properties) is selected for further investigation. Similarly, the case of rotational speed of 1000 rpm and variable traverse speeds is selected for further investigation on the microhardness distribution.

Figure 4.14 and 4.15 shows the Vickers hardness profile across the centerline of friction stir weldments of the second group (under different tool rotational speeds) and the third group (at different traverse speeds). It's clearly observed that the maximum hardness across the centerline of all the weldements is found to be at the HAZ/TMAZ interface zone of the aluminum alloy 2024-T3, while there is a significant hardness decrease at the HAZ/TMAZ interface zone of the aluminum alloy 6061-T6 and that conforms to the results of J.H. Ouyang and R. Kovacevic (2001). Generally the hardness of the nugget zone did not show a significant decrease compared with the base alloys. The hardness of the base alloy of 2024-T3 was recorded to be about 136HV20 while the hardness of the base alloy of 6061-T6 was recorded to be about 95HV20. The minimum hardness recorded for the nugget zone and for the HAZ/TMAZ interface for 6061 alloy for a rotational speed of 600 rpm were recorded as 94HV20 and 58HV20 respectively. The maximum hardness recorded for the nugget zone and HAZ/TMAZ interface for 2024 alloy with rotational speed of 1000 rpm were 128HV20 and 119HV20 respectively. For a constant traverse speed of 50 mm/min, the nugget zone hardness value has shown an increase with the increasing in the rotational speed from 600 to 1000rpm (exept one condition as seen in figure 4.11 which is representing in the 1200 rpm that is show decreasing). On the other hand the nugget zone hardness has shown only a slight

change with varying traverse speed while keeping the rotational speed constant at 1000 rpm. A relatively stable (and maximum) hardness value of nearly 125HV20 value was obtained at rotational speed of 1000 rpm and traverse speed of 50 mm/min across the centerline of the weldement.

The hardness variations in the longitudinal section of the dissimilar metal welds are related to the different aluminum alloy structure caused mainly by the material flow and heat action created under the stirring action.

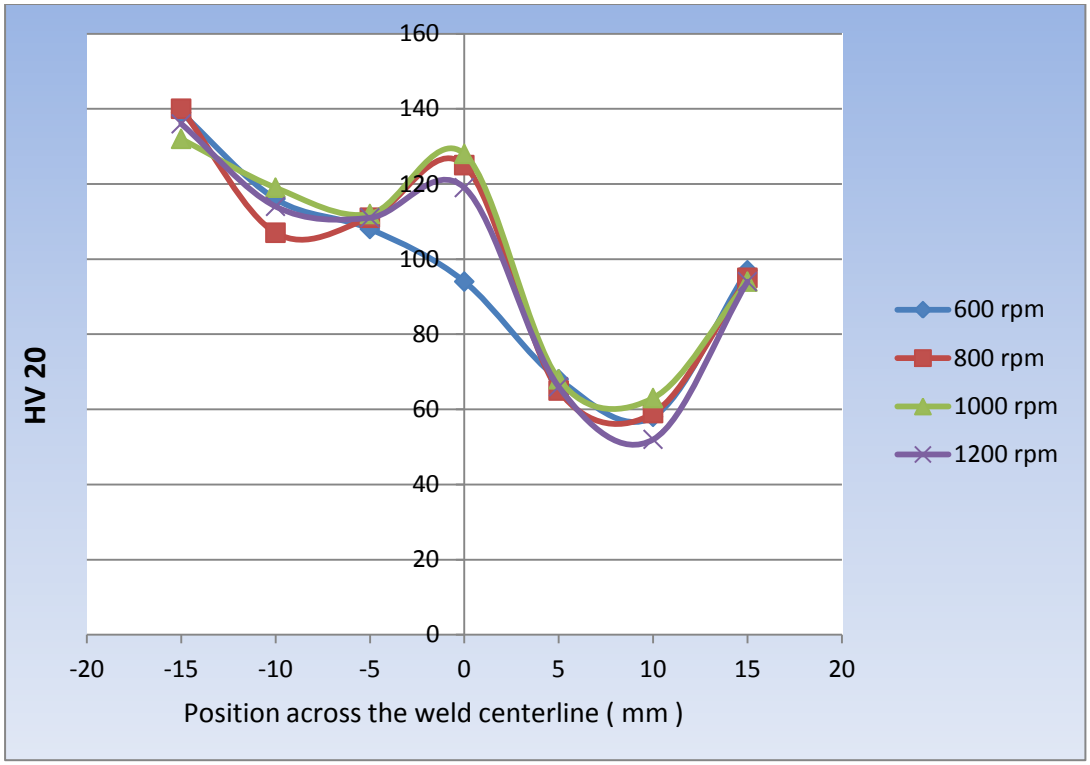

Figure 4.14 Vickers hardness profile across the weld centerline of friction stir welded Al alloy for different tool rotation and constant travel speed of 50 mm/min

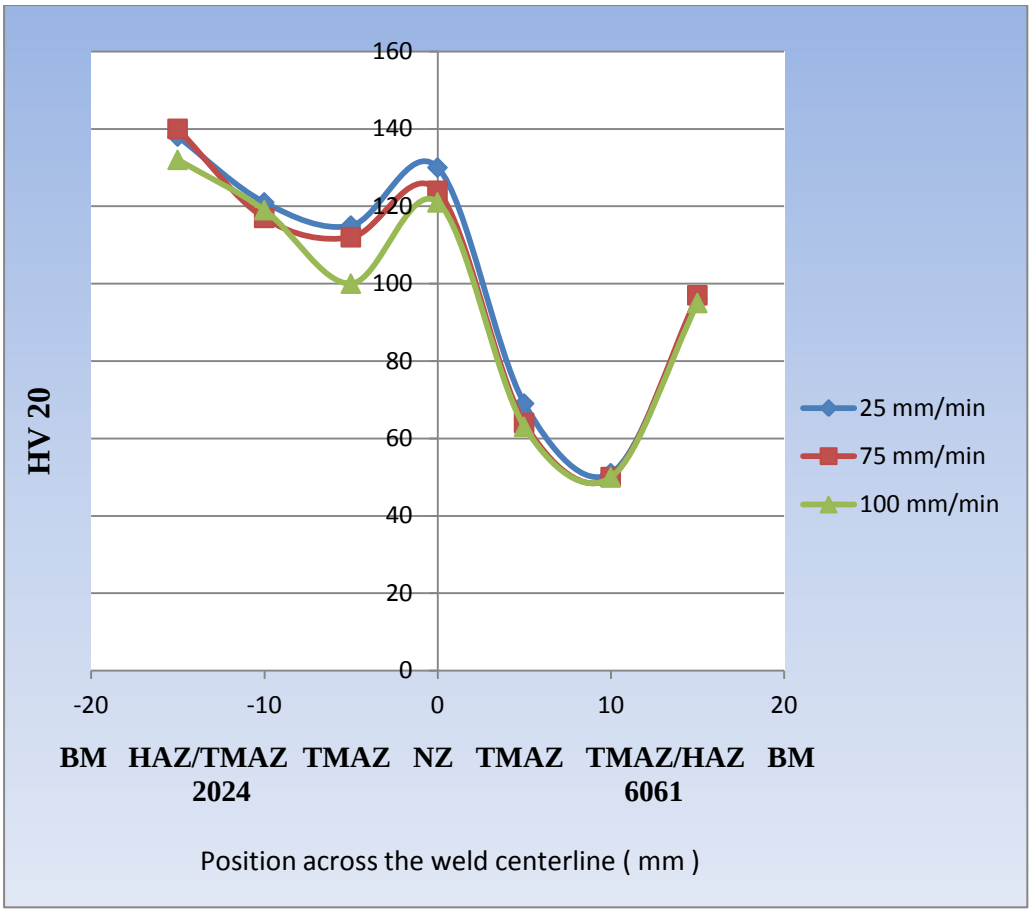

Figure 4.15 Vickers hardness profile across the weld centerline of friction stir welded Al alloy for different travel speeds and constant rotation speed of 1000 rpm

It is assumed that the hardness of the weld nugget depends on the grain size of the nugget zone as well as on the dissolution of strengthening precipitation during the thermal cycle of the FSW. Increasing tool rotational speed leads to an increase of the nugget zone temperature and consequently dissolution of the strengthening precipitates will take place for more regions, then after, reprecipitation and natural ageing take place during the cooling of the weld leading to the recovery of the hardness in the weld area and the adjacent areas where dissolution temperature has reached.

The plastic deformation alter the precipitation sequence in a number of ways, either by heterogeneous precipitation on dislocation sites or by modification of bulk

precipitation kinetics. Hence the precipitation behavior in the alloy 2024 is expected to differ from what is usually happening in the 6061 alloy, so that the hardness profile which is a good measure of the mechanical properties of the weld area showing different behavior due the different mechanisms for microstructural developments. The concurrency of strain hardening, reprecipitation and grain size refining at the nugget zone may all be responsible of the high hardness of the nugget zone of joints . Moreover, the HAZ in the advancing side of the weld is found to be slightly wider than that of the retreating side due to the fact that the advancing side of the weld is influenced by higher heat input because of greater relative velocity between the tool and the work piece in this side.

Vickers hardness variations of friction stir welding for the variable rotational and traverse speeds are summarized in the tables 4.5 (a) and (b) respectively.

Table 4.5 (a) Microhardness distribution results of the weldments for the case of using variable rotational speeds at a constant traverse speed (AA6061-T6 on advancing side)

Rotation speed	**Traverse speed**	**BM or HAZ**	**HAZ/TMAZ**	**TMAZ**	**NZ**	**TMAZ**	**TMAZ/HAZ**	**BM or HAZ**
600	50	139	116	108	94	68	58	97
800		140	107	111	125	65	59	95
1000		132	119	112	128	68	63	94
1200		136	114	111	119	66	52	94

Table 4.5 (b) Microhardness distribution results of the weldments for the case of using variable traverse speeds at a constant rotational speed (AA6061-T6 on advancing side)

Traverse speed	**Rotation speed**	**BM or HAZ**	**HAZ/TMAZ**	**TMAZ**	**NZ**	**TMAZ**	**TMAZ/HAZ**	**BM or HAZ**
25	1000	138	121	115	130	69	51	96
75		140	117	112	124	64	50	97
100		132	119	100	121	63	50	95

4.8 Effect of welding conditions on microstructural features of the weld area.

Transverse macro-sections through the welds revealed the characteristic features of friction stir welds in dissimilar aluminum alloys. A typical cross-section of the defect free friction stir weld is shown in figure 4.16. It is contain the nugget zone (NZ) in the form of fine recrystallized grains surrounded by a region of heavily deformed grains referred to the thermomechanically affected zone (TMAZ), and beyond these the heat affect zone (HAZ) which receives only the heat of friction and the parent metal (BM) which keeps the properties of the initial condition of the alloy. As the joint is done between dissimilar alloys, therefore, each side will have the below regions which is considered differ from the other. The advancing side and the retreating side of the joints are denoted by AS and RS respectively.

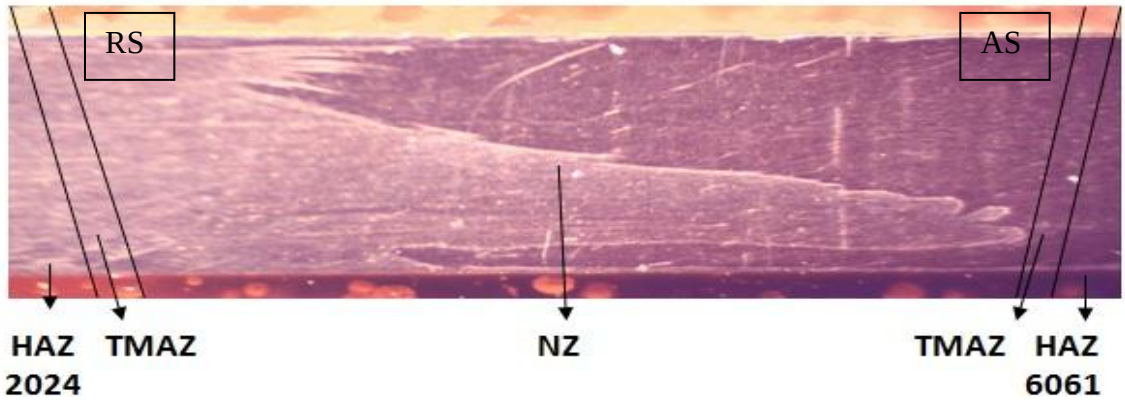

Figure 4.16 Macrographic of FSW of the dissimilar joint showing macrostructural zones

Optical microscopic examination was carried out on joints welded with traverse speed of 50 mm/min and variable rotational speed of 600 , 800 , 1000 and 1200 rpm as illustrated in figure 4.17, then the same examination was repeated on the joints of rotational speed of 1000 rpm and variable traverse speed of 25 , 75 , 100 mm/min as shown in figure 4.18. The optical microscope illustrated that no defects (porosity or kissing bond) exist in the stirred zones for the most joints produced. Figure 4.17 and 4.18 shows the typical features of the different zones in a dissimilar weld cross section of aluminum alloys 2024-T3 to 6061-T6 including the nugget zone and the thermomechanically affected zones and also the heat affected zones for both alloys and shows the effect of rotational speed and traverse speed on the material flow and mechanical mixing behavior. The asymmetric pattern of material flow can be observed clearly in the nugget zones for all of the weldements. The bonding between the alloys is clearly complete instead of the incomplete alternate mixing in the dissimilar metal welds. The nugget zone is composed of three different regions of strong plastic deformation and material flow of both Al-alloys which are classified by the mechanically mixed region (MMR) which is represented by the scattered particles of different alloys, the stirring induced plastic flow region (SPFR) featured

by the alternative vortex-like lamellae of the both aluminum alloys and the unmixed region (UMR) consisting of fine equiaxed grains. Increasing the rotational speed make the material flow stronger. Also a severe plastic deformation occurred along the top surface of the weld due to the contact of the tool shoulder with the workpiece. The horizontal flow along the shoulder surface is called the Surface flow and the inward flow in the interior portion of the nugget is called the return flow.

Surface flow pushes the plasticized material down into the weld cavity, while the return flow has an upward flow tendency due to the resistance to material flow in the retreating side. The effectiveness of shoulder flow becomes greater as the tool rotational speed is increased which pushes more material to flow into the weld cavity due to the increased heat flow from the tool shoulder. But the effectiveness of tool shoulder gradually decreases as the tool traveling increases and at very high tool traveling; it seems that most of the heat flow comes from the friction of the tool pin, and consequently pin driven flow is dominant and therefore there is more tendency to the formation of void defects or reducing the weld quality as it is illustrated in the tensile test results. It has been considered that the friction heat flow is a very important factor for friction stir welding because the microstructure in the stir zone is strongly influenced by the friction heat flow. There are two main mechanisms for friction heat flow during FSW. One is the friction heat flow from the shoulder, and the other is that from the pin.When the rotational speed is increased from 600 to 1200 rpm, the return material flow penetrates wider into the 6061-Al alloy side of the nugget zone. At rotational speed 600 rpm, material flow is slow and discontinuous across the line of joint. Because the heats resulting from the rotating tool do not produce enough temperature needed for softening the surrounding

materials. At rotational speed 1200 rpm, a larger mechanically mixing and faster material flow can be found in the nugget zone.

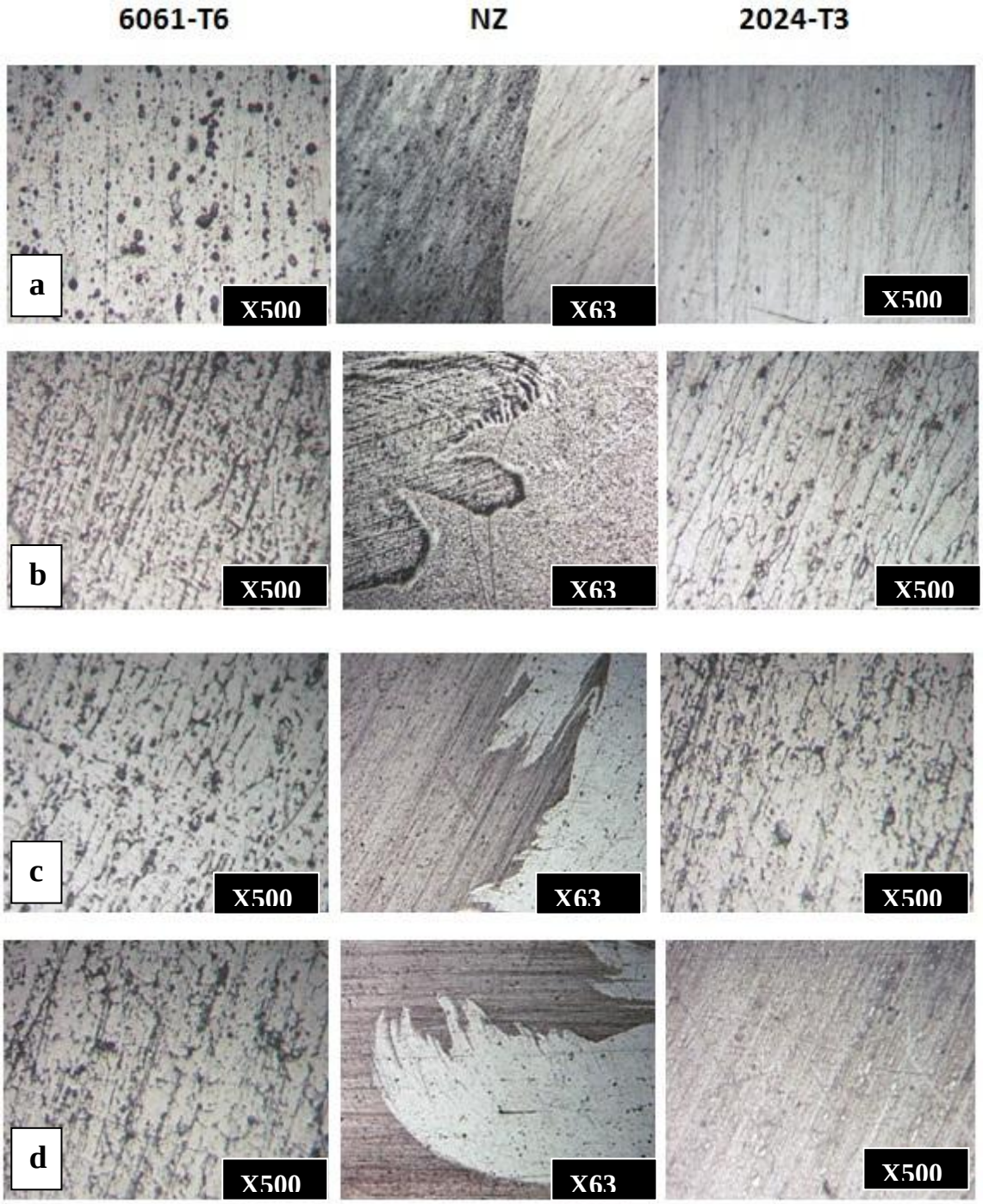

Figure 4.17 Optical macro and micrographs on a transverse section through a friction stir welded dissimilar alloys 2024-T3 and 6061-T6 at rotational speed of (a) 600 rpm, (b) 800 rpm, (c) 1000 rpm & (d) 1200 rpm at a constant traverse speed of 50 mm/min

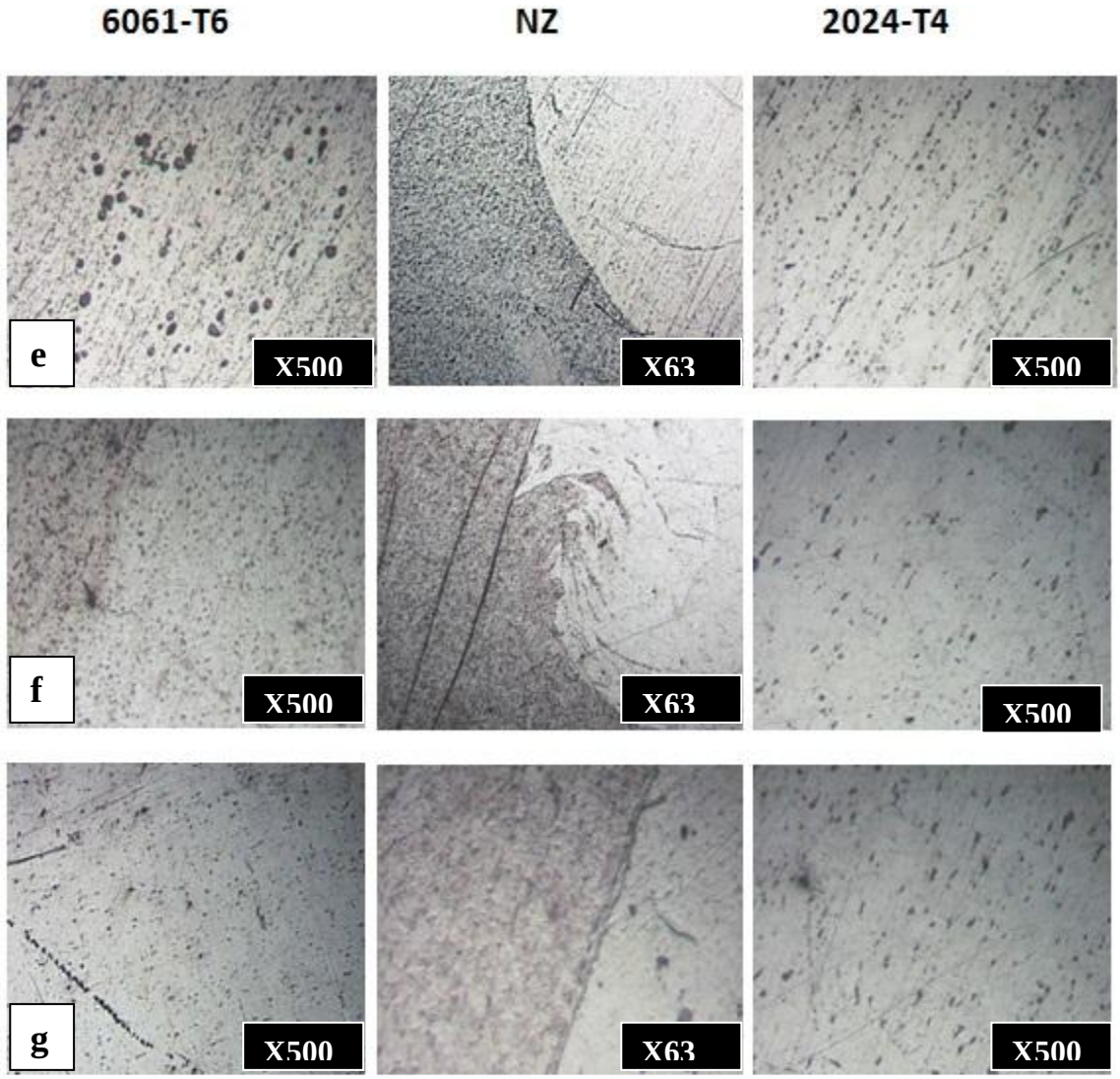

Figure 4.18 Optical macro and micrographs on a transverse section through a friction stir welded dissimilar alloys 2024-T3 and 6061-T6 at traverse speed of, (e) 25 mm/min, (f) 75 mm/min & (g) 100 mm/min at a constant rotational speed of 1000 mm/min

Figure 4.18 show the effect of the welding speed on the material flow and mechanical mixing in the dissimilar alloys. At welding speed of 25 mm/min, the mechanical mixing becomes more uniform in compare with the welding speed of 100 mm/min. The material flow is steady and asymmetric.

It's clear from figure 4.19, that the grain size within the weld nugget many times smaller than that of the parent metal due to the dynamic recrystallization associated with friction stir welding. The average sizes of the grains within the weld zone of friction stir welding of aluminum alloys 2024-T3 to 6061-T6 is ranging from 1 to 10 μm.

Dynamic recrystallization of the nugget area is considered as the most significant features of FSW process which occurs due to the fact that this area is subjected to the largest amount of plastic strain and the highest temperature.

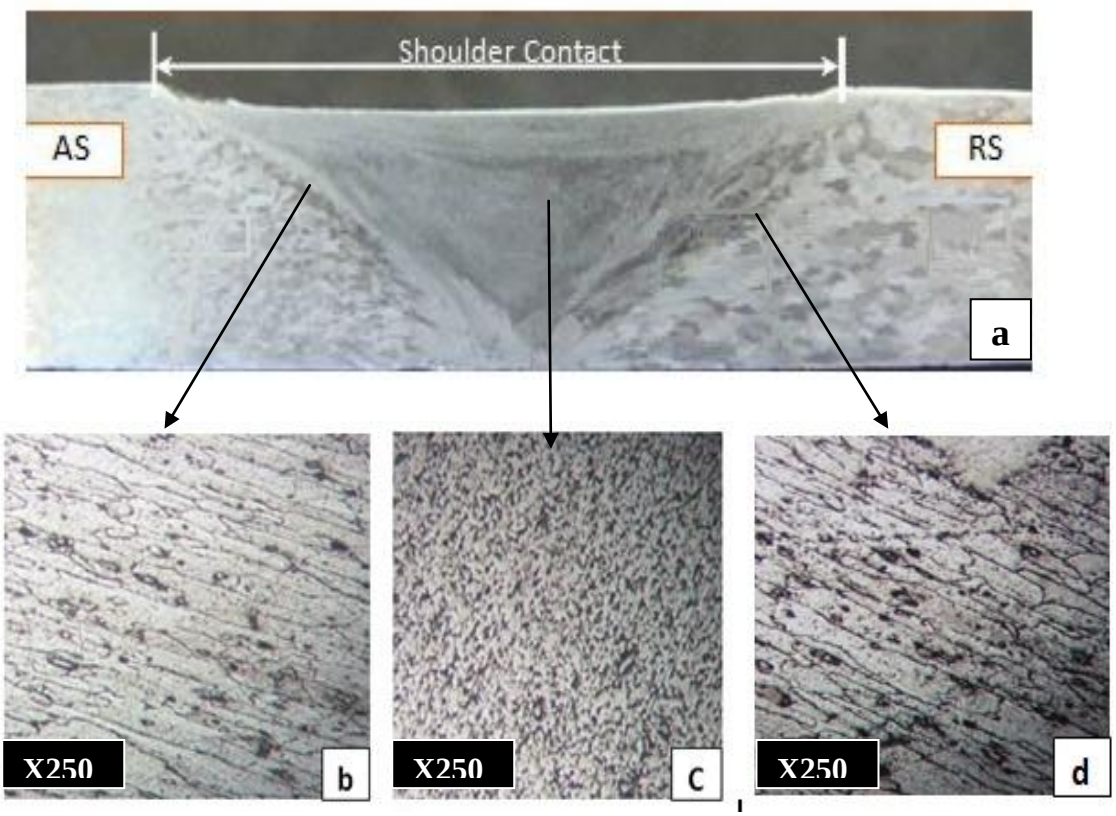

Figure 4.19 FSW macro and microstructure comparisons of 2024-T3 and 6061-T6 (a) cross-sectional view of the weld, (b) base plate grain structure of 2024-T3, (c) grain structure of the nugget zone & (d) base plate grain structure of 6061-T6

In the thermomechanically affected zone (TMAZ), the material flow produced by welding can be observed. The initial grains are rotated in the TMAZ and the recrystallization begins at the TMAZ / NZ interface. The borderline between the TMAZ of the advancing side and weld nugget is apparently visible because grains or deformation bands in the TMAZ have flowed only a little into the region behind the tool, leaving a fairly sharp interface between NZ and TMAZ. While on the retreating side, such flow is greater because the rotating tool shears metal from before it to that side and additionally sweeps it into the region behind resulting in a very irregular interface between the elongated TMAZ grains and the equiaxed nugget grains [28]. The TMAZ is a transition region between the heat affected zone (HAZ) and the weld nugget characterized by partial recrystallization progress. It can be seen from this illustration that the relationship between tool rotational and travel speeds able to prevent the occurrence of microscopic welding defects, largely depends on the material being welded. The formation such defects in friction stir welding depends basically on the selected process parameters such tool rotation and travel speeds and tool design related features and can be explained by the basic mechanics of FSW. The tool generates friction heat and causes a significant plastic deformation of material. The weld is formed by forging the plasticized material into the cavity behind the tool from the retreating side RS to the advancing side AS. When FSW is performed at a higher speed, the material receives less work per unit of the weld length, i.e. fewer tool rotations per tool travel (rev/mm). Under such conditions, the plasticized material may be cooler, and less easily forged by the tool, resulting in voids remaining unconsolidated in the advancing side.

CHAPTER 5

CONCLUSIONS

5.1 Conclusion

In this thesis, friction stir welding of dissimilar aluminum alloys 2024-T3 to 6061-T6 was studied in Gaziantep University, BCS metal company by using a vertical milling machine with a variable rotational and transverse speeds to show the effect of process parameters on the mechanical and microstructural properties and then analysis the results to satisfy the optimum condition by using mechanical and microstructural tests. The following conclusions are obtained from this study:

1. The experimental results show that the weldments indicated no visible defects, weld surface is even and uniform with better surface appearance and without any pores and discontinuities for the interior portion.
2. The better strength of the weldements (220 MPa) is achieved when the aluminum alloy 6061-T6 located on the advancing side using rotational speed of 1000 rpm and travel speed of 50 mm/min.
3. For all of the process parameters, fracture occurred on the side of the aluminum alloy 6061-T6 which is considered as the weakest alloy in compare with the 2024-T3 alloy due to its lower ultimate tensile strength.
4. When the aluminum alloy 6061-T6 located on the retreating side, fracture occurred at the NZ/TMAZ interface. While when it was located on the advancing side, fracture occurred at the HAZ/TMAZ interface.

5. Low ductility and bending properties was observed when the aluminum alloy 6061 located at the retreating side, while better ductility and bending properties with no crack or defects achieved when the aluminum alloy 6061 located at the advancing side which is show 180 degree.
6. For the hardness distribution the maximum value for the nugget zone was 128HV20 representing the better welding condition of 1000 rpm rotation speed and 50 mm/min travel speed. In addition, maximum value of hardness distribution for the nugget zone recorded at traverse speed of 25 mm/min.
7. When the rotational speed is increased from 600 to 1200 rpm, the return material flow penetrates wider into the 6061-Al alloy side of the nugget zone.

5.2 Recommendation for future study

1. Investigating stress corrosion cracking susceptibility of friction stir welding of dissimilar aluminum alloys 2024-T3 and 6061-T6.
2. Investigating fatigue behavior of friction stir welded joints.
3. Using experimental and finite element modeling for computing residual stresses in friction stir weldments.
4. Using finite element modeling to better understand the material flow, the heat transfer and the difference between advancing side and retreating side during friction stir welding.
5. Studying the effect of variable tool design i.e. the geometrical parameters on the friction stir welding of dissimilar aluminum alloys 2024-T3 and 6061-T6.

REFERENCES

Wayne Thomas and Pedro Vilaca. (2011). Friction stir welding technology . *Springer-Verlag Berlin Heidelberg*.

Akinlabi and Esther Titilayo. (2010). Characterization of dissimilar friction stir welds between 5754 aluminum alloy and C11000 Copper . *Nelson Mandela Metropolitan University.*

C. J. Dawes, The Welding Institute, Abington Hall, Cambridge adapted for TALAT by Roy Woodward, Birmingham and Christian Leroy, EAA. (1999). Friction stir welding. *Copyright TWI*.

L.Boehm. (2004). New engineering process in aircraft construction : application of laser-beam and friction stir welding. *Original Russian text copyright,* vol.31.no.1. pp.27-29.

J. Norberto Pires. et al. (2006). Welding Robots Technology ,System Issues and Applications. PhD Thesis © *Springer-Verlag London Limited*.

Calvin Blignault. et al. (2002). Design, Development and Analysis of the Friction Stir Welding Process. *Msc Thesis, electrical, industrial & mechanical engineering Port Elizabeth Technikone.*

Gene Mathers. (2002). The welding of aluminum and its alloy, *Woodhead Publishing ltd*. PP.161-165.

R.S. Mishra. (2005). Friction stir welding and processing *Journal of Center for Friction Stir Processing, Department of Materials Science and Engineering, University of Missouri, Rolla, MO 65409, USA.*

K. Kumar, Satish V. Kailas. (2007). The role of friction stir welding tool on material flow and weld formation . *Ph.D. Dissertation, Civil Engineering Department, Colorado State University, Fort Collins, Colorado, USA.*

P. Kah. et. al. (2009). Experimental investigation of welding of aluminum alloys profiles and wrought plate by FSW. *Lappeenranta University of Technology, Lappeenranta, Finland*.

Terry Khaled. (2005). An outsider looks at friction stir welding *Ph.D. Chief Scientific / Technical Advisor, Metallurgy Federal Aviation Administration 3960 Paramount Boulevard. Lakewood, CA 90712 (562) 627-5267.*

R.Rai. et. al. (2011). Review: friction stir welding tools. *Science and Technology of Welding and Joining. Science and Technology of Welding and Joining.* Vol.16, No. 4.

Kazuhiro Nakata. et. al. (2000). Weldability of High Strength aluminum alloys by friction stir welding. Joining and Welding Research Institute, Osaka University, Mihogaoka, Ibaraki, Osaka 567-0047 Japan. ISIJ International, Vol. 40. pp. S15-sl 19.

Bahemmat et al. (2008). Experemental study on the effect of rotational speed and tool pin profile on AA2024 aluminum friction stir welded butt joints. *ASME Early Career Technical Conference, Miami, Florida, USA.*

Sutton M. A. et al. **(**2001). Microstructural studies of friction stir welds in 2024-T3 aluminum. *Department of Mechanical Engineering, Uni_ersity of South Carolina,* 300 *Main Street, Columbia, SC* 29208, *USA. Materials Science and Engineering A323 (2002) 160–166.*

Hakan Aydin, et. al. (2008). Tensile properties of friction stir welded joints of 2024 aluminum alloys in different heat treated state. *journal of materials and design*.

P. Cavaliere. (2008). Effect of welding parameters on mechanical and microstructural properties of dissimilar AA6082–AA2024 joints produced by friction stir welding . *Department of ‘‘Ingegneria dell’Innovazione”, Engineering Faculty, University of Salento, Via per Arnesano, I-73100 Lecce, Italy. Materials and Design 30 (2009) 609–616.*

M. Vural. Et. al. (2007). On the friction stir welding of aluminium alloys EN AW 2024-0 and EN AW 5754-H22. *International Scientific Journal. Volume 28.*

Saad and Toshiya. (2007). Microstructure and Mechanical Properties of Friction Stir Welded Dissimilar Aluminum Joints of AA2024-T3 and AA7075-T6. *Joining and*

Welding Research Institute, Osaka University, Ibaraki 567-0047, Japan, Materials Transactions, Vol. 48, No. 7.

Y. J. CHAO et. al. (2001). Effect of Friction Stir Welding on Dynamic Properties of AA2024-T3 and AA7075-T7351. *the Department of Mechanical Engineering, University of South Carolina, Columbia, S.C.*

Won-Bae Lee. Et. al. (2004). Mechanical Properties Related to Microstructural Variation of 6061 Al Alloy Joints by Friction Stir Welding. *Department of Advanced Materials Engineering, Sungkyunkwan University, 300 Cheoncheon-dong, Jangan-gu, Suwon, Kyounggi-do 440-746, Korea*, Materials Transactions, Vol. 45, No. 5.

M. A. Abdelrahman. Et. al. (2012). The effect of FSW tool geometry on AA6061-T6 weldments . *Metallurgy Department, Nuclear Research Center, Atomic Energy Authority, Cairo, Egypt . Arab Journal of Nuclear Sciences and Applications, 45(2)407-418.*

F.C. LIU and Z.Y. MA. (2008). Influence of Tool Dimension and Welding Parameters on Microstructure and Mechanical Properties of Friction-Stir-Welded 6061-T651 Aluminum Alloy . *The Minerals, Metals & Materials Society and ASM International.*

N. T. Kumbhar and K. Bhanumurthy. (2008). Friction Stir Welding of Al 6061 Alloy . *Materials Science Division Bhabha Atomic Research Centre Trombay, Mumbai - 400085. India* . Asian J. Exp. Sci., vol. 22, No. 2, 63-74.

Indira Rani M. et. al. (2011). a study of process parameters of friction stir welded AA 6061 aluminum alloy in 0 and T6 conditions . *Mechanical Engineering Department, JNTUH CE, Hyderabad, India . ARPN Journal of Engineering and Applied Sciences* . vol. 6, No. 2.

Huijie LIU. et. al. (2005). friction stir weldabilities of AA1050-H24 and 6061-T6 aluminum alloys . *national key laboratory of advanced welding production technology , harbin institute of technology , harbin 150001, china*. J. master. Sci. technology, vol.21 , No.3.

Muhamad Tehyo. et. al. (2012). Influence of friction stir welding parameters on metallurgical and mechanical properties of dissimilar joint between semi-solid metal 356-T6 and aluminum alloys 6061-T651. *Department of Industrial Engineering, Faculty of Engineering, Princess of Naradhiwas University, Mueang, Narathiwat, 96000 Thailand.* Songklanakarin J. Sci. Technol.

M. Ghosh. et. al. (2010). Optimization of friction stir welding parameters for dissimilar aluminum alloys . *Materials Science and Technology Division, National Metallurgical Laboratory (CSIR), Jamshedpur 831 007, India* . Materials and Design 31 (2010) 3033–3037.

W H Jiang and R Kovacevic. (2004). Feasibility study of friction stir welding of 6061-T6 aluminium alloy with AISI 1018 steel . *Research Centre for Advanced Manufacturing, Southern Methodist University, Richardson, Texas, USA* . Proc. Instn Mech. Engrs vol. 218 Part B.

Ki-Sang Bang. et. al. (2011). Interfacial Microstructure and Mechanical Properties of Dissimilar Friction Stir Welds between 6061-T6 Aluminum and Ti-6%Al-4%V Alloys. *Automotive Components Center, Korea Institute of Industrial Technology, Korea 1110-9 Oryong-dong, Buk-gu, Gwangju 500-480, Korea . Materials Transactions,* vol. 52, No. 5 pp. 974 to 978.

P M G P Moreira . et. al. (2004). Friction stir welds of dissimilar aluminium alloys AA6061-T6 and AA6082-T6 . *FEUP – Faculty of Engineering, University of Porto, R. Dr. Roberto Frias, 4200-465 Porto, Portugal.*

Ying Li. (1999). Flow visualization and residual microstructures associated with the friction-stir welding of 2024 aluminum to 6061 aluminum. *Department of Metallurgical and Materials Engineering, The Uni*6*ersity of Texas at El Paso, El Paso, TX* 79968, *USA* . Materials Science and Engineering A271 213–223.

J.H. Ouyang and R. Kovacevic. (2001). Material Flow and Microstructure in the Friction Stir But Welds of the Same and Dissimilar Aluminum Alloys. *Research Center for Advanced Manufacturing, Department of Mechanical Engineering, Southern Methodist University, 1500 International Parkway, Suite 100, Richardson, TX 75081.* Journal of Materials Engineering and Performance . vol 11(1).

Wiliam D. Callister, Jr. (2001). Fundamentals of materials science and engineering. *Department of metallurgical engineering , the university of Utah*.

APPENDIX A

The certificate of chemical composition

الشركة العامة للفحص والتأهيل الهندسي S.I.E.R
قسم المختبرات والفحص الهندسي.Lab. & E..I . Dep

الجهة المـستفيدة : السيد نزار مضر عبد الودود
رقم امـــر العمل : ----/ 2012
الـــــتاريـــــخ : 28 / 1 / 2013
نوع النمـــوذج : plate

Certificate

1-Chemical composition:

Sample	Si%	Fe%	Cu%	Mn%	Mg%	Cr%	Ni%	Zn%	Ti%	Pb%	Sn%	V%	AL%
Plate T= 3mm	0.125	0.272	4.19	0.614	1.26	0.012	0.010	0.165	0.018	0.009	0.005	0.000	Bal.

2-Type of metal: ----------

ملاحظات:.
- النتيجة تخص النموذج المفحوص فقط.
- تم الفحص بدرجة حرارة $23^{o}C$ ونسبة الرطوبة % 80 .

الشركة العامة للفحص والتأهيل الهندسي
المختبرات والفحص الهندسي
Lab. & Insp.
١/٢٨

و/رئيس قسم المختبرات والفحص الهندسي
م.ارس طالب

LI-1 Issue 4(Jun.12)

Element concentration of aluminum alloy 2024

SPECTRO

10/01/2013 09:24:37

Method: Al-30 F

10/01/2013 09:24:28

Comment: Al/Cu -alloy

Element concentration

Sample Name:

	Si	Fe	Cu	Mn	Mg	Cr	Ni	Zn
	%	%	%	%	%	%	%	%
Ø (4)	0.125	0.272	4.19	0.614	1.26	0.012	0.010	0.165

	Ti	Ag	Be	Bi	Cd	Co	Li	Pb
	%	%	%	%	%	%	%	%
Ø (4)	0.018	0.00059	0.00038	0.0090	0.00032	< 0.0010	0.00032	0.009

	Sn	V	Zr	Al
	%	%	%	%
Ø (4)	0.005	0.000	0.004	93.4

Element concentration of aluminum alloy 6061

SPECTRO

10/01/2013 10:02:00

Method: Al-01 F

Comment: Al -global

Element concentration

10/01/2013 10:01:56

Sample Name:

	Si	Fe	Cu	Mn	Mg	Cr	Ni	Zn
	%	%	%	%	%	%	%	%
1	0.676	0.608	0.325	0.0671	1.02	0.197	0.0137	0.109
2	0.670	0.572	0.327	0.0659	1.04	0.194	0.0131	0.106
Ø (2)	**0.673**	**0.590**	**0.326**	**0.0665**	**1.03**	**0.196**	**0.0134**	**0.108**
sd	0.0048	0.0253	0.0013	0.00084	0.0114	0.0021	0.00043	0.0020
rsd	0.7	4.3	0.4	1.3	1.1	1.1	3.2	1.9

	Ti	Ag	B	Be	Bi	Ca	Cd	Co
	%	%	%	%	%	%	%	%
1	0.0157	< 0.00010	0.0032	0.00013	0.0056	0.0020	0.00015	< 0.0010
2	0.0157	< 0.00010	0.0030	0.00024	0.0065	0.0020	0.00014	< 0.0010
Ø (2)	**0.0157**	**< 0.00010**	**0.0031**	**0.00019**	**0.0061**	**0.0020**	**0.00014**	**< 0.0010**
sd	0.00001	0.00000	0.00010	0.00008	0.00063	0.00001	0.00000	0.00000
rsd	0.1	0.0	3.2	40.5	10.4	0.4	3.0	0.0

	Hg	La	Li	Na	P	Pb	Sn	Sr
	%	%	%	%	%	%	%	%
1	< 0.0020	< 0.00050	< 0.00020	< 0.00010	0.0027	0.0095	< 0.0010	< 0.00010
2	< 0.0020	< 0.00050	< 0.00020	< 0.00010	0.0031	0.0092	< 0.0010	< 0.00010
Ø (2)	**< 0.0020**	**< 0.00050**	**< 0.00020**	**< 0.00010**	**0.0029**	**0.0093**	**< 0.0010**	**< 0.00010**
sd	0.00000	0.00000	0.00000	0.00000	0.00033	0.00021	0.00000	0.00000
rsd	0.0	0.0	0.0	0.0	11.3	2.2	0.0	0.0

	V	Zr	Al
	%	%	%
1	0.0096	0.0029	96.9
2	0.0096	0.0029	97.0
Ø (2)	**0.0096**	**0.0029**	**96.9**
sd	0.00002	0.00007	0.0220
rsd	0.2	2.3	0.0

APPENDIX B

Radiographic test report of first sample

جمهورية العراق
وزارة الصناعة والمعادن
الشركة العامة للفحص والتأهيل الهندسي(المعهد سابقا)
(شركة عامة)

العـــــدد: 10
التاريخ : 2013/01/27

Order No.

Radiographic Test Report
تقرير التصوير الشعاعي

Client						Film Type	D7
Project	Friction Welding					IQI	ASTM 1A
App. Code	ASME IIIV					Source	X-ray generator
Page	1		Of	1		FFD	700mm
Exposure	Kv	180	mA	5	Time	15 Sec	

No.	Joint No.	Material	Dia.	Welder	Kind of defect	Evaluation			Remark
						Acc.	Not Acc.	Acc. After Repair	
1	1	Al	N/A		NSD	√			
2									
3									
4									
5									
6									
7									
8									
9									
10									
11									
12									
13									
14									
15									
16									
17									
18									
19									

101- Longitudinal Crack
102- Transverse Crack
106- Branching Crack
2011-Gas Pore
2013- Localized (clustered) porosity
2014- Linear Porosity
FD- Film defect

3011- Slag Lines
3012- Slag Inclusion
304- metallic Inclusion
401-Lack of penetration
402-lack of fusion
2015- Elongated Porosity
N S D : No Significant Discontinuities.

5011-Undercut (continuous)
5012- Undercut(interrupted)
514- Irregular surface
504- Excessive penetration
5041- Local Excessive penetration
610 – Oxidized Root

Technician
Akram Yousif

Evaluated By
Mawloodd D. Alwan

Approved By

Name	Aws Talib
Date	28-1-2013

LI-51 Issue 4(Mar.12)

Radiographic test report of all the samples

جمهورية العراق
وزارة الصناعة والمعادن
الشركة العامة للفحص والتأهيل الهندسي(المعهد سابقا)
(شركة عامة)

العـــدد: 118
التاريخ : 2013/3/10

Order No.

Radiographic Test Report

تقرير التصوير الشعاعي

Clint	Nazar mudher					Film Type	D4
Project	Friction Stir Welding					IQI	DIN62
App. Code	ASME IIIV					Source	X-RAY generator
Page	1		Of	1		FFD	600mm
Exposure	Kv	150	mA	2	Time	1min	

No.	Joint No.	Material	THK mm	Welder	Kind of defect	Evaluation			Remark
						Acc.	Not Acc.	Acc. After Repair	
1	Group1 AS1	AL	3		NSD	*			
2	Group1 AS2	AL	3		NSD	*			
3	Group1 AS3	AL	3		NSD	*			
4	Group1 AS4	AL	3		NSD	*			
5	Group2 AS5	AL	3		NSD	*			
6	Group2 AS6	AL	3		NSD	*			
7	Group2 AS7	AL	3		NSD	*			
8	Group2 AS8	AL	3		NSD	*			
9									
10									
11									
12									
13									
14									
15									
16									
17									
18									
19									

101- Longitudinal Crack
102- Transverse Crack
106- Branching Crack
2011-Gas Pore
2013- Localized (clustered) porosity
2014- Linear Porosity
FD- Film defect

3011- Slag Lines
3012- Slag Inclusion
304- metallic Inclusion
401-Lack of penetration
402-lack of fusion
2015- Elongated Porosity
NSD: No Significant Discontinuities

5011-Undercut (continuous)
5012- Undercut(interrupted)
514- Irregular surface
504- Excessive penetration
5041- Local Excessive penetration
610 – Oxidized Root

Technician
Akram yousif

Evaluated By
Husam A. Zaya

Approved By

Name	Aws Talib
Date	10/3/2013

LI-51 Issue 4(Mar.12)